This is to certify that the

thesis entitled

TE WAVE EXCITATION AND SCATTERING ON
ASYMMETRIC PLANAR DIELECTRIC WAVEGUIDE

presented by

Boutheina Kzadri

has been accepted towards fulfillment
of the requirements for

M.S. degree in Elect. Eng.

Dennis P. Nyquist
Major professor

Date July 19, 1989

TE WAVE EXCITATION AND SCATTERING ON ASYMMETRIC PLANAR DIELECTRIC WAVEGUIDE

By

Boutheina Kzadri

A THESIS

Submitted to
Michigan State University
in partial fulfillment of the requirements
for the degree of

MASTER OF SCIENCE

Department of Electrical Engineering and Systems Science

1989

ABSTRACT

TE WAVE EXCITATION AND SCATTERING ON ASYMMETRIC PLANAR DIELECTRIC WAVEGUIDE

By

Boutheina Kzadri

An asymmetric planar dielectric waveguide is formed by the tri-layered substrate/film/cover environment, typical of integrated circuits for millimeter and optical wavelengths. The structure supports surface waves when the film-layer guiding region has positive index contrast relative to its surround. An electric Green's function (believed new) is constructed for the TE field maintained in the film layer by currents immersed in that region. Using a direct complex analysis approach, the Green's function is expanded in the discrete and continuous propagation spectrum components for the asymmetric planar waveguide. The electric Green's function is exploited to study scattering of TE surface waves by dielectric obstacles in the film layer.

If the y-axis is normal to the layer interfaces and the waveguiding z-axis is parallel to them, then an x-invariant TE field, having only an x component, is excited by the similar component of current. Spectral analysis in the axial transform domain leads to

$$E_x(y,z) = \int_{LCS} G(y|y';z-z')\, J_x(y',z')\, dy'dz'$$

where LCS designates the longitudinal cross section of the source region and the Green's function has a spectral integral representation. Subsequent to complex transform plane analysis, $G(y|y';z-z')$ is

decomposed into the superposition of a discrete surface wave, arising from pole singularities, and a radiative component arising from integrations about substrate/cover branch cuts. If a dielectric discontinuity having index contrast $\delta n^2 = n_d^2(y,z) - n_f^2$ is immersed in the film layer, an excess polarization current is excited and maintains a scattered field. This current is proportional to the product of the induced field and the refractive index contrast. Within the obstacle the total field $\vec{E} = \vec{E}^i + \vec{E}^s$ consists of the impressed field of an incident wave augmented by the scattered field. Rearranging leads to the EFIE

$$E_x(y,z) - j\omega\varepsilon_0 \int_{LCS} \delta n^2(y',z')\ G(y|y';z-z')E_x(y,z)dy'dz' = E_x^i(y,z)$$

A pulse-Galerkin's solution leads to the induced field, from which scattering coefficients are calculated. Extensive numerical results for various obstacle configurations will be presented.

TO MY PARENTS

ACKNOWLEDGMENTS

The author wishes to express special thanks to Dennis P. Nyquist for his help and guidance in this research.

TABLE OF CONTENTS

LIST OF FIGURES

Chapter One

INTRODUCTION

The subject of planar integrated optical circuits is of increasing interest. An asymmetric planar dielectric waveguide is formed by a tri-layered substrate/film/cover environment, typical of integrated circuits for millimeter and optical wavelengths. This thesis is intended to construct an electric Green's function (believed new) for the TE field maintained by currents immersed either in the film or the cover layer. The electric Green's function is exploited to study scattering of TE surface waves by dielectric obstacles in the film layer.

Discontinuities in dielectric waveguides are assuming increasing importance in the design and development of optical and millimeter wave components. A discontinuity problem arises in the splicing of two dielectric waveguides and is relevant to inter-device coupling in millimeter and optical integrated circuits. Various methods have been presented recently by several authors for the analysis of discontinuity problem in slab waveguides [1,2,3,4,5,6]. Analysis of longitudinal discontinuities in dielectric slab waveguides was treated by Uzunoglo [5]. His approach was relevant to the symmetric slab waveguide. Moreover, he exploited Sommerfeld integrals to formulate the electric Green's function for the TE field in the film layer.

This thesis uses a direct complex analysis approach to construct the Green's function which is represented by a 1-D spectral integral. The second chapter contains a general statement of the equations governing fields and Hertz potentials in the asymmetric tri-layered environment of Figure 1. A Hertz potential Green's function for the tri-layered background is developed for sources immersed in either the cover or the film layer. It will be shown that the Hertz potential Green's function decomposes into a reflected part augmented by a primary component. Due to the x-invariance of the fields, this Green's function is represented by a 1-D spectral integral instead of a 2-D integral [6].

The propagation mode spectrum is treated in chapter three. A discrete spectrum is found to be associated with surface waves, while superposition of the continuous spectrum yields the radiation field. A polarization EFIE description of slice discontinuities along the asymmetric slab guiding region is developed in chapter four. Method of moment (MoM) numerical solutions are obtained for the discontinuity field, leading to scattering coefficients and radiated power.

Some words about notation here might be helpful. As a convention, upper case letters denote space domain quantities, while their transform domain counterparts are designated by lower case letters. The symbol $\jmath$ denotes the elementary imaginary number, while j denotes the current density in the transform domain. Finally, the following assumptions are valid throughout the thesis:

(1) All media are linear and isotropic unless otherwise specified.

(2) An $\exp(\jmath\omega t)$ time dependence is assumed for the electromagnetic fields and is suppressed.

(3) All media are non-magnetic with permeability μ_o.

Chapter Two

ELECTROMAGNETICS OF ASYMMETRIC LAYERED DIELECTRICS

2.1 INTRODUCTION

This chapter is devoted to the evaluation of electromagnetic fields in the tri-layered environment of Figure 1. The electric field in the system is expressed in terms of the electric source density maintaining the fields, integrated into an appropriate Green 's function. Details of the development of the Green 's function for the layered structure of Figure 1 will be established. In fact, knowledge of this specialized Green's function is of primary importance, since it will be used later in this thesis to formulate the integral equation for the electric field within discontinuities immersed in the layered dielectric environment.

Analysis of electromagnetic fields in a layered environment was first made by Sommerfeld [7] in 1909. The first problem attacked by Sommerfeld was that of electric dipoles oriented normal or tangential to an air-earth interface. Integral-transform techniques were used to obtain integral representations for the fields produced by former dipoles. These integral expressions are known as Sommerfeld integrals.

The tri-layered environment, typical of integrated circuits at millimeter and optical wavelengths, is depicted in Figure 1. A uniform dielectric guiding region (film layer) of refractive index n_f occupies the region $-t < y < 0$; it is immersed between a substrate region ($y < -t$) with refractive index n_s, and a cover surround which fills the space $y > 0$ and is characterized by a refractive index n_c. All dielectric media are assumed to possess limitingly small dissipation with $Re\{n_f\} > Re\{n_s\} > Re\{n_c\}$, where $Re\{\cdot\}$ designates the real part of the quantity within the braces. The electric current density immersed in the film region is parallel to the x-axis so it only maintains TE polarized electromagnetic fields in all three regions.

In the next section, the electric Hertzian potential $\vec{\Pi}$ for the tri-layered structure is formulated as a convolution of the impressed current density $\vec{J}$ with an appropriate Green's function. The development of the Green's function will be detailed. In section 3, a physical interpretation will be given to explain the y dependence of all the terms present in the expression for the Green's function.

2.2 HERTZIAN POTENTIAL GREEN'S FUNCTION

Details of the relationship of the Hertz potential to the electric field, along with the Helmholtz equation for the potential, is reviewed in Appendix A.

Development of general dyadic electric Green's functions for layered structures has been presented by Bagby and Nyquist [8]. The electric field Green's dyads are found in terms of associated Hertzian potential Green's dyads, developed by an extension of Sommerfeld's classic method [9]. The Hertzian potential dyadic Green's function was shown to have scalar components expressed as 2-D spatial frequency integrals of the Sommerfeld type. In the subsequent development, the analysis in [8] is specialized for the tri-layered structure of Figure 1. Using the TE symmetry where the fields are invariant with respect to x, the Green's function will have only one component expressed in 1-D

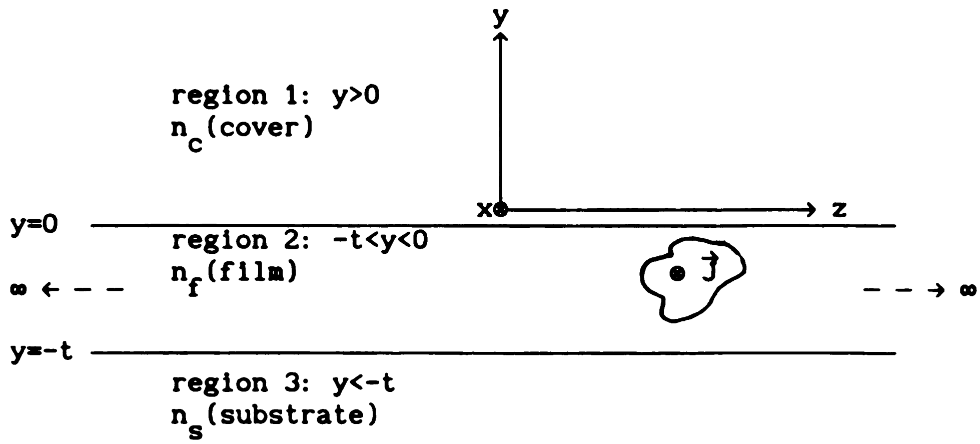

(a) Sources in the film

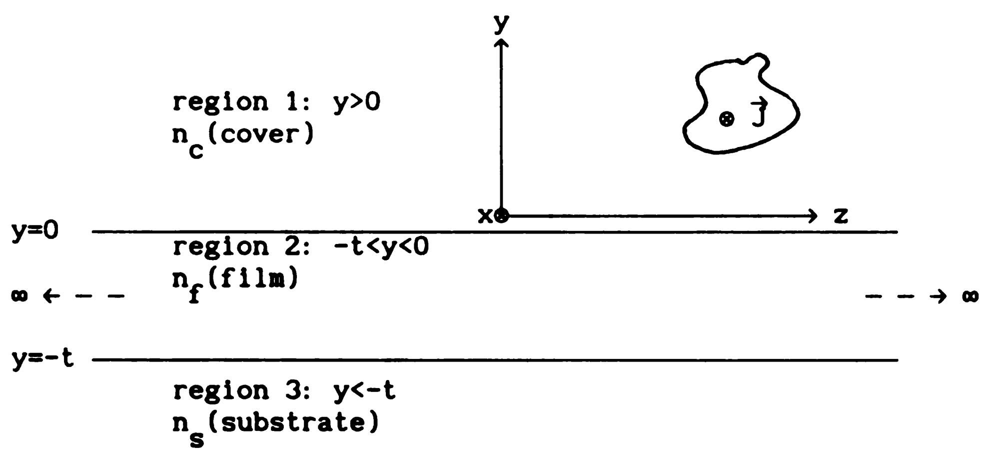

(b) Sources in cover

Figure 1: Tri-layered structure used as the background environment for integrated circuits.

spectral integral representation.

2.2.1 Axial Transform Domain Field Equations

Consider the situation depicted in Figure 1. An impressed current $\vec{J}$ parallel to the x-axis (or an impressed polarization $\vec{P} = \vec{J}/j\omega$) radiates in the film or cover region, generating electric Hertzian potential in each region of the tri-layered structure. The relations that relate the electric field and the magnetic field to the Hertz potential are

$$\vec{E}_\ell = (k_\ell^2 + \nabla\nabla\cdot)\,\vec{\Pi}_\ell \tag{2.1}$$

$$\vec{H}_\ell = j\omega\varepsilon_\ell \nabla \times \vec{\Pi}_\ell \tag{2.2}$$

The Hertzian potentials satisfy the following Helmholtz equation

$$(\nabla^2 + k_\ell^2)\,\vec{\Pi}_\ell = \begin{cases} -\vec{J}/j\omega\varepsilon_1 & ,\ell=1 \\ 0 & ,\ell\neq 1 \end{cases} \tag{2.3}$$

in each region (ℓ=s,f,c for substrate, film, cover). Equation (2.3) is solved for the potential by Fourier transformation on spatial variables tangential to the layer interfaces. Axial uniformity along the waveguiding axis (i.e $\varepsilon\neq\varepsilon(z)$ and $\mu\neq\mu(z)$) prompts Fourier transformation on that axial variable. Define the axial transform pair $F(z) \leftrightarrow f(\zeta)$ where $F(\cdot)$ and $f(\cdot)$ denote

$$f(\zeta) = \int_{-\infty}^{+\infty} F(z)\, e^{-j\zeta z} dz$$

$$F(z) = \frac{1}{2\pi}\int_{-\infty}^{+\infty} f(\zeta)\, e^{j\zeta z} d\zeta$$

As a convention, upper case letters denote space-domain quantities, while their transform-domain counterparts are designated by lower case letters. Taking Fourier transforms of equations (2.1) through (2.3) yields

$$\vec{e}_\ell = (k_\ell^2 + \tilde{\nabla}\tilde{\nabla}\cdot)\ \vec{\pi}_\ell$$

$$\vec{h}_\ell = j\omega\varepsilon_\ell\ \tilde{\nabla}\times\vec{\pi}_\ell \tag{2.5}$$

$$\left(\frac{\partial^2}{\partial y^2} - p_\ell^2\right)\vec{\pi}_\ell = \begin{cases} \dfrac{-\vec{J}}{j\omega\varepsilon_i} & ,\ell=i \\ 0 & ,\ell\neq i \end{cases} \tag{2.6}$$

where $p_\ell^2 = \zeta^2 - k_\ell^2$ and $\tilde{\nabla}$ denotes $\nabla_t + \hat{z}j\zeta$ and $\nabla_t = \hat{y}\frac{\partial}{\partial y}$ since we have invariance with respect to x (i.e $\frac{\partial}{\partial x} = 0$) . Since the electric current density $\vec{J}$ is x-directed, it maintains similar Hertzian potential ($\vec{\Pi} = \hat{x}\Pi_x$) and hence $\tilde{\nabla}.\vec{\pi} = 0$. Equations (2.4) and (2.5) are reduced to

$$\vec{e}_\ell = \hat{x}\ k_\ell^2 \pi_{x\ell} \tag{2.7}$$

$$\vec{h}_\ell = j\omega\varepsilon_\ell\left(\frac{\partial}{\partial y}\ \hat{y} + \hat{z}j\zeta\right)\times\ \hat{x}\ \pi_{x\ell} = j\omega\varepsilon_\ell\left(-\hat{z}\frac{\partial\pi_{x\ell}}{\partial y} + \hat{y}j\zeta\pi_{x\ell}\right) \tag{2.8}$$

2.2.2 Green's Function Decomposition ; Primary Component

The total potential in each layer is the sum of a primary part $\vec{\pi}^p$ and a scattered part $\vec{\pi}^s$; the primary potential propagates directly from the source to a field point in either the cover or film layer, whereas the scattered potential arrives at a field point after being scattered (reflected or transmitted) from cover and/or film interfaces. The transform-domain primary potential $\vec{\pi}^p$ in either the cover or film region satisfies the inhomogeneous Helmholtz equation (2.6) in the transform domain (2.6). That is

$$\left(\frac{\partial^2}{\partial y^2} - p_\ell^2\right) \pi^s_{x\ell}(y,\zeta) = 0 \tag{2.9}$$

and
$$\left(\frac{\partial^2}{\partial y^2} - p_i^2\right) \pi^p_{xi}(y,\zeta) = \frac{-j_x}{j\omega\varepsilon_i} \tag{2.10}$$

where i = c for sources in the cover and i = f for sources in the film. Equation (2.9) has solution

$$\pi^s_{x\ell} = w^s_{x\ell}(\zeta)\, e^{\pm p_\ell y}$$

where the coefficient $w^s_{x\ell}(\zeta)$ is determined by application of appropriate boundary conditions. The solution for the primary potential in either the cover or the film region in terms of the impressed current in the transform domain is

$$\pi^p_{xi}(y,\zeta) = \int_{-\infty}^{+\infty} \frac{j_x(y',\zeta)}{j\omega\varepsilon_i}\, g^p_i(y|y';\zeta\,)\, dy' \tag{2.11}$$

where the transform domain primary Green's function is determined in Appendix B and found to be

$$g_i^P(y|y';\zeta) = \frac{e^{-p_i|y-y'|}}{2p_i}$$

Since the transformed current is given by

$$j_x = \int_{-\infty}^{+\infty} J_x(y',z')\, e^{-j\zeta z'} dz' \tag{2.12}$$

inversion of the transformed primary potential may be performed and yields the particular solution to (2.3) with the primary potential in either the cover or the film region given by

$$\Pi_{xi}^P(y,z) = \frac{1}{2\pi} \int_{-\infty}^{+\infty} \pi_{xi}^P(y,\zeta)\, e^{j\zeta z}\, d\zeta$$

Replacing the expression of $\pi_{xi}^P(y,\zeta)$ with that of equation (2.11) and writing the expression for the transformed current as in (2.12) the principal potential in spatial domain may be expressed as

$$\Pi_{xi}^P(y,z) = \frac{1}{2\pi} \int_{-\infty}^{+\infty} d\zeta \iint_{LCS} \frac{J_x(y',z')}{j\omega\varepsilon_i}\, g_i^P(y/y';\zeta)\, e^{j\zeta(z-z')} dy'dz' \tag{2.13a}$$

where LCS designates the longitudinal cross section of the dielectric layer where the current is immersed. Interchanging the spatial integration with the spectral integration, (2.13a) becomes

$$\Pi^{p}_{xi}(y,z) = \iint_{LCS} \frac{J_x(y',z')}{j\omega\varepsilon_i} G^{p}_{i}(y|y';z-z')\ dy'dz' \tag{2.13}$$

where the space domain Green's function $G^{p}_{i}(y|y';z-z')$ is given by

$$G^{p}_{i}(y|y';z-z') = \frac{1}{2\pi} \int_{-\infty}^{+\infty} g^{p}_{i}(y|y',\zeta)\ e^{j\zeta(z-z')}\ d\zeta \tag{2.14}$$

2.2.3 Reflected Green's Function for Sources in the Film Layer

Consider the situation shown in Figure 2. Electric current density, immersed in the film region, maintains EM fields in each region. Solution to the homogeneous Helmholtz equation (2.9) in the transform domain gives the scattered potential in each layer as:

$$\pi^{s}_{x\ell}(y,\zeta) = w^{s}_{x\ell}(\zeta)\ e^{\pm\, p_\ell y}$$

where $\pi^{s}_{x\ell}(y,\zeta)$ is representative of either a reflected potential $\pi^{r}_{x}(y,\zeta)$ or a transmitted potential $\pi^{t}_{x}(y,\zeta)$. Therefore in the cover region ($y > 0$), the scattered wave is in the form of a transmitted wave travelling in the upward direction ($+\hat{y}$)

$$\pi^{t}_{xc}(y,\zeta) = w^{t}_{xc}(\zeta)\ e^{-p_c(\zeta)y}$$

Similarly, in the substrate region ($y < -t$) the scattered potential is given by

$$\pi^{t}_{xs}(y,\zeta) = w^{t}_{xs}(\zeta)\ e^{+p_s(\zeta)y}$$

which consists of a wave travelling in the downward direction. Finally, in the film region $(-t < y < 0)$ the transformed scattered potential consists of two reflected waves from the adjacent interfaces propagating upward and downward. Hence we have

$$\pi^r_{xf}(y,\zeta) = w^{r+}_{xf}(\zeta)e^{-p_f(\zeta)y} + w^{r-}_{xf}(\zeta)e^{+p_f(\zeta)y} \tag{2.15}$$

where w^{r+}_{xf} and w^{r-}_{xf} designate the coefficients associated with a wave travelling upward and downward, respectively. The coefficients w^t_{xc}, w^t_{xs} w^{r+}_{xf} and w^{r-}_{xf} are determined by satisfying appropriate boundary conditions [8] across the dielectric interfaces. Note that in writing the expressions for the above potentials in each region, radiation conditions as $y \longrightarrow \pm \infty$ has been taken into account. In fact, for the transverse wave number $p^2_\ell = \zeta^2 - k^2_\ell$, the branch that leads to outward-propagating or attenuated waves must be chosen . This requires that $Re\{p_\ell\} > 0$ and $Im\{p_\ell\} > 0$. The appropriate boundary conditions are adapted from Sommerfeld's [7] development of Hertzian potential boundary conditions. Enforcing continuity of tangential $\vec{e}$ at the interfaces requires

$$\pi_{xc}(o,\zeta) = N^2_{fc}\pi_{xf}(o,\zeta)$$

and

$$\pi_{xf}(-t,\zeta) = N^2_{sf}\pi_{xs}(-t,\zeta)$$

where N^2_{fc} and N^2_{sf} are the ratio of the film permittivity to the cover permittivity and the ratio of the substrate permittivity to the film permittivity, respectively. In a similar fashion, continuity of

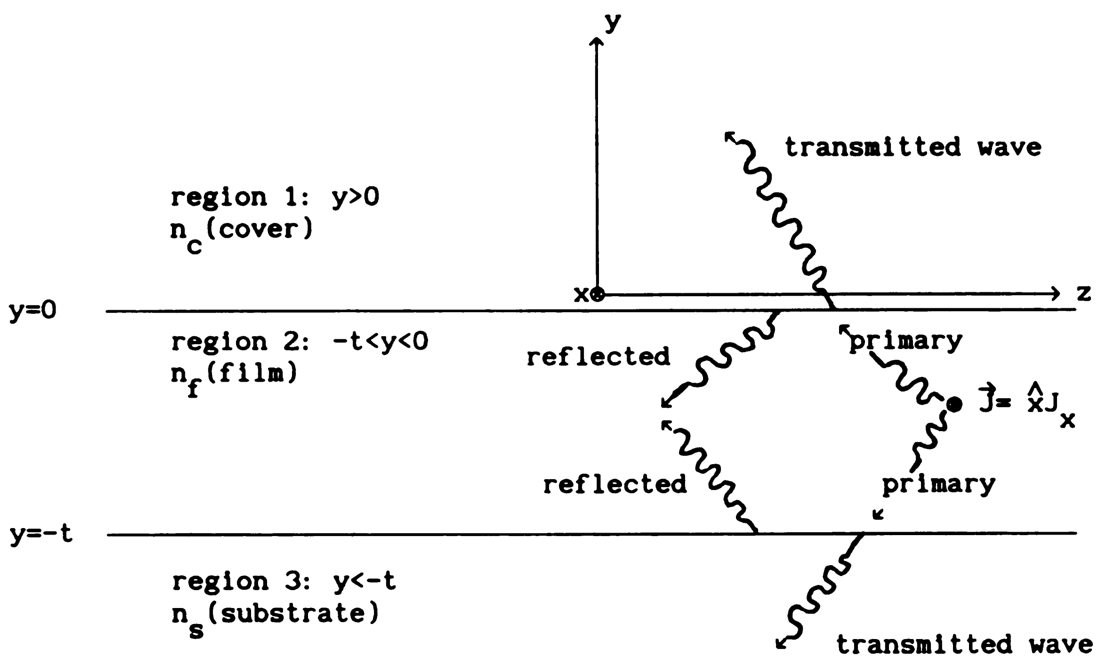

Figure 2: Primary and scattered-waves in the tri-layered structure with current immersed in the film.

tangential $\vec{H}$ yields

$$\frac{\partial \pi_{xc}(o,\zeta)}{\partial y} = N_{fc}^{2}\frac{\partial \pi_{xf}(o,\zeta)}{\partial y}$$

$$\frac{\partial \pi_{xf}(-t,\zeta)}{\partial y} = N_{sf}^{2}\frac{\partial \pi_{xs}(-t,\zeta)}{\partial y}$$

where $\pi_{x\ell}$ denotes the total Hertzian potential (primary plus scattered) in the ℓ'th region (ℓ=c,s,f for cover, substrate and film). Note that the primary Hertz potential is present only in the film region, produced by current density immersed in that layer.

Application of the above boundary conditions to determine w_{xf}^{r+} and w_{xf}^{r-} is detailed in Appendix C. The results are as follows

$$w_{xf}^{r+} = \int_{-\infty}^{+\infty}\frac{j_x(y'\zeta)}{2j\omega\varepsilon p_f}\,(R_{+}^{(1)}e^{-p_f(y'+2t)} + R_{+}^{(2)}e^{p_f(y'-2t)})\;dy'$$

and

$$w_{xf}^{r-} = \int_{-\infty}^{+\infty}\frac{j_x(y'\zeta)}{2j\omega\varepsilon_f p_f}\,(R_{-}^{(1)}e^{-p_f(y'+2t)} + R_{-}^{(2)}e^{p_f y'})\;dy'$$

where the reflection coefficients $R_{+}^{(1)}$, $R_{+}^{(2)}$, $R_{-}^{(1)}$ and $R_{-}^{(2)}$ are given as

$$R_{+}^{(1)} = \frac{(p_f+p_c)(p_f-p_s)\; e^{p_f t}}{2\cosh(p_f t)\;[(p_f^2+p_c p_s)\tanh(p_f t)+p_f(p_s+p_c)]}$$

$$R_{+}^{(2)} = \frac{(p_f-p_s)(p_f-p_c)\; e^{p_f t}}{2\cosh(p_f t)\;[(p_f^2+p_c p_s)\tanh(p_f t)+p_f(p_s+p_c)]}$$

$$R_{-}^{(1)} = R_{+}^{(2)}$$

$$R_{-}^{(2)} = \frac{(p_f+p_s)(p_f-p_c)\; e^{p_f t}}{2\cosh(p_f t)\;[(p_f^2+p_c p_s)\tanh(p_f t)+p_f(p_s+p_c)]}$$

Exploiting the expressions for w_{xf}^{r+} and w_{xf}^{r-} in equation (2.15) yields

$$\pi_{xf}^{r}(y,\zeta) = \int_{-\infty}^{+\infty} \frac{j_x(y',\zeta)}{j\omega\varepsilon_f}\, g_f^{r}(y|y';\zeta)dy'$$

where the axial Fourier transform reflected Green's function is expressed as

$$g_f^{r}(y|y';\zeta) = \frac{1}{2p_f}\Big[R_{+}^{(1)} e^{-p_f(y+y'+2t)} + R_{+}^{(2)} e^{-p_f(y-y'+2t)} + R_{-}^{(1)} e^{p_f(y-y'-2t)} + R_{-}^{(2)} e^{p_f(y+y')} \Big] \qquad (2.16)$$

Proceeding in the same fashion as for the primary Hertz potential, the spatial domain reflected Hertz potential is given as

$$\Pi^{r}_{xf}(y,z) = \iint\limits_{-\infty}^{+\infty} \frac{J_x(y',z')}{j\omega\varepsilon_f} G^{r}_{f}(y|y';z-z')\, dy'dz' \tag{2.17}$$

where the spatial domain reflected Green's function is expressed as

$$G^{r}_{f}(y|y';z-z') = \frac{1}{2\pi} \int_{-\infty}^{+\infty} g^{r}_{f}(y|y';\zeta) e^{j\zeta(z-z')} d\zeta \tag{2.18}$$

Finally, the total Hertz potential in the film layer is the sum consisting of a primary wave augmented by a scattered wave and given as

$$\Pi_{xf}(y,z) = \iint\limits_{-\infty}^{+\infty} \frac{J_x(y',z')}{j\omega\varepsilon_f} G_{f}(y|y';z-z')\, dy'dz' \tag{2.19}$$

where the total Green's function consists of a primary part augmented by a reflected one and is expressed as

$$G_{f}(y|y';z-z') = G^{p}_{f}(y|y';z-z') + G^{r}_{f}(y|y';z-z') \tag{2.20}$$

2.2.4 Reflected Green's Function for Sources in the Cover Layer

In this section, the procedure of determining the reflected Green's function is outlined for the situation depicted in Figure 3. Source and field points are situated in the cover region. The primary wave is reflected or transmitted at the film-cover interface. The reflected wave in the cover travels in the positive y direction while the transmitted wave in the film layer propagates in the negative y

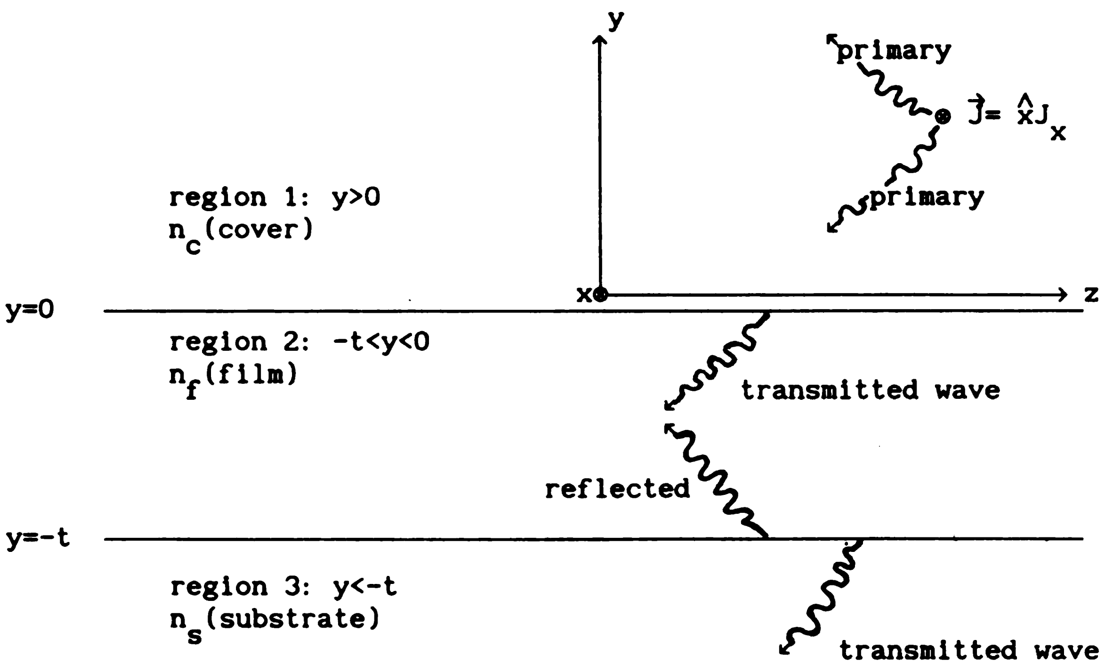

Figure 3: Primary and scattered-waves in the tri-layered structure with current immersed in the cover

direction. Intuitively, the y-dependent part of the reflected wave should have a phase of $y+y'$. In fact, the reflected Green's function for sources in the cover layer is given as

$$G_c^r(y|y';z-z') = \frac{1}{2\pi}\int_{-\infty}^{+\infty} g_c^r(y|y';\zeta)e^{j\zeta(z-z')}d\zeta \tag{2.21}$$

where the transform domain reflected Green's function $g_c^r(y|y';\zeta)$ is expressed as

$$g_c^r(y|y';\zeta) = \frac{R(\zeta)e^{-p_c(y+y')}}{2p_c(\zeta)} \tag{2.22}$$

The reflection coefficient $R(\zeta)$ is given as

$$R(\zeta) = \frac{p_f(p_c-p_s)+(p_cp_s-p_f^2)\tanh(p_ft)}{p_f(p_s+p_c)+(p_cp_s+p_f^2)\tanh(p_ft)}$$

Outlined below is a simple procedure for obtaining the above reflected Green's function

1. Solutions to the homogeneous Helmholtz equation (2.9) determines the scattered potential in each layer as $\pi_{x\ell}^s(y,\zeta) = w_{x\ell}^s(\zeta)e^{\pm p_\ell y}$ which represents either a reflected wave or a transmitted wave.

2. Taking into account the radiation condition stated earlier, the potential in the film region consists of standing waves

$$\pi_{xf}^t(y,\zeta) = w_{xf}^{t-}(\zeta)e^{p_f(\zeta)y} + w_{xf}^{t+}(\zeta)e^{-p_f(\zeta)y}$$

The potential in the cover region consists of a reflected wave traveling in the positive y direction and given as

$$\pi^{r}_{xc}(y,\zeta) = w^{r}_{xc}(\zeta)e^{-p_c(\zeta)y} \tag{2.23}$$

hence the total potential in the cover region is

$$\pi_{xc}(y,\zeta) = \pi^{r}_{xc}(y,\zeta) + \pi^{p}_{xc}(y,\zeta)$$

The potential in the substrate region consists of a transmitted wave propagating in -y direction

$$\pi^{t}_{xs} = w^{t}_{xs}(\zeta)e^{p_s y}$$

3. The coefficients w^{r}_{xc}, w^{t+}_{xf}, w^{t-}_{xf} and w^{t}_{xs} are determined by satisfying appropriate boundary conditions at the cover-film interface and at the film-substrate interface. Those boundary conditions are expressed as

$$\pi_{xc}(o,\zeta) = N^2_{fc}\pi_{xf}(o,\zeta)$$

$$\pi_{xf}(-t,\zeta) = N^2_{sf}\pi_{xs}(-t,\zeta)$$

$$\frac{\partial\pi_{xc}(o,\zeta)}{\partial y} = N^2_{fc}\frac{\partial\pi_{xf}(o,\zeta)}{\partial y}$$

$$\frac{\partial\pi_{xf}(-t,\zeta)}{\partial y} = N^2_{sf}\frac{\partial\pi_{xs}(-t,\zeta)}{\partial y}$$

where $\pi_{x\ell}$ denotes the total transformed Hertzian potential (primary plus scattered). Hence the result is

$$w^{r}_{xc}(\zeta) = \int_{\infty}^{\infty} \frac{j_x(y',\zeta)}{2j\omega\varepsilon_c p_c} R(\zeta)e^{-p_c y'}dy'$$

4. Exploiting the expressions for $w^{r}_{xc}(\zeta)$ in equation (2.23) yields

$$\pi^{r}_{xc}(y,\zeta) = \int_{-\infty}^{\infty} \frac{J_x(y',\zeta)}{2j\omega\varepsilon_c p_c} R(\zeta) e^{-p_c(y+y')} dy'$$

5. Proceeding in the same fashion as for the primary Hertzian potential, the spatial domain reflected Hertz potential in the cover region is expressed as

$$\Pi^{r}_{xc}(y,z) = \iint_{-\infty}^{\infty} \frac{J_x(y',z')}{j\omega\varepsilon_c} G^{r}_{c}(y|y';z-z')\, dy'dz'$$

Finally, the total spatial domain hertz potential in the cover layer consists of the sum of a reflected wave and a principal wave. It is expressed in terms of the spatial domain Green's function as

$$\Pi^{r}_{xc}(y,z) = \iint_{-\infty}^{\infty} \frac{J_x(y',z')}{j\omega\varepsilon_c} G_c(y|y';z-z')\, dy'dz'$$

where

$$G_c(y|y';z-z') = \frac{1}{2\pi} \int_{-\infty}^{\infty} \frac{1}{2p_c} \left\{ e^{-p_c|y-y'|} + R(\zeta)\, e^{-p_c(y+y')} \right\} d\zeta \tag{2.24}$$

2.3 A PHYSICAL INTERPRETATION

As seen In Figure 2, a source point at y' produces a primary disturbance in the film region which consists of a wave propagating in either ±y direction. In either case, the primary wave is reflected or transmitted at the cover-film interface and at the film-substrate

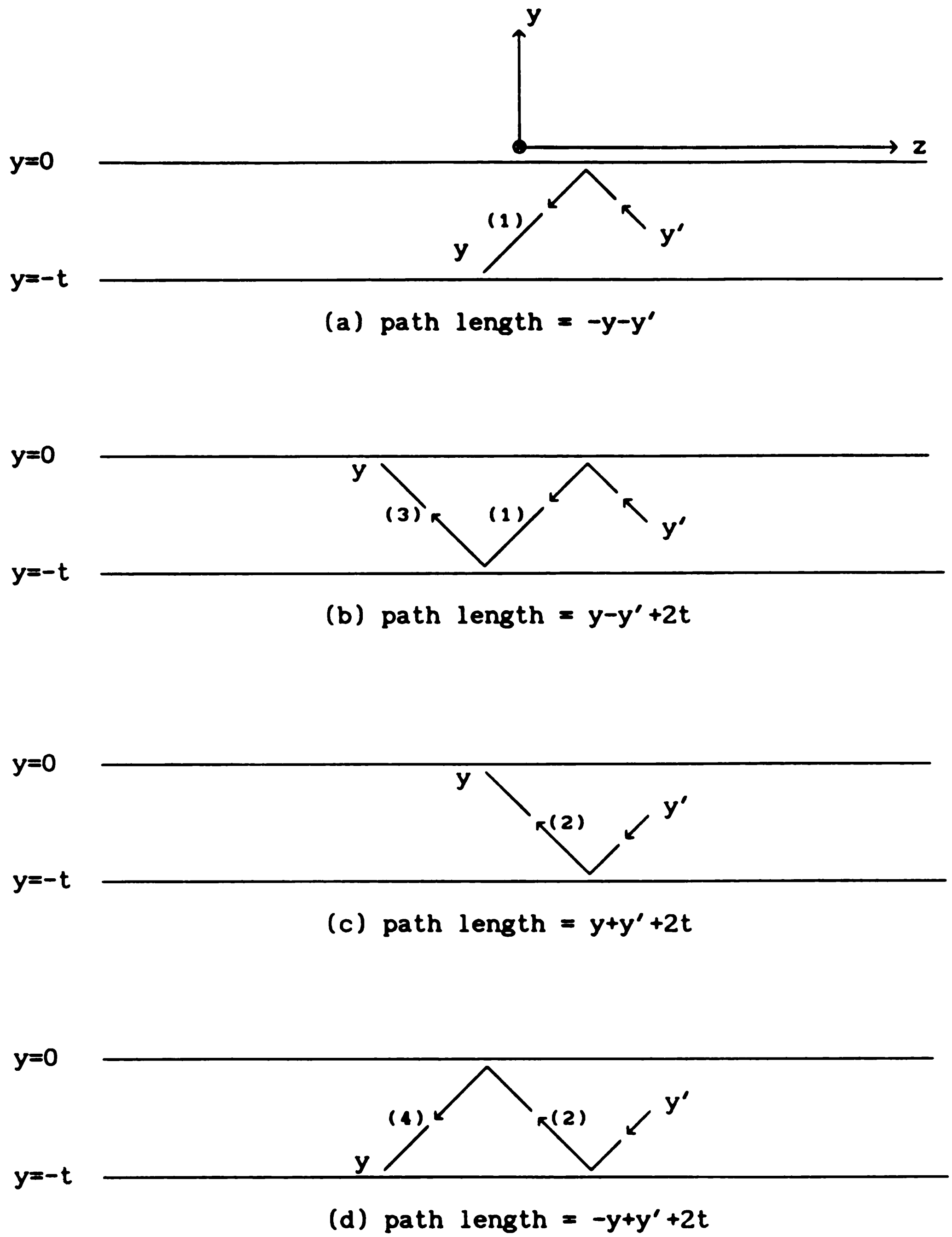

Figure 4: The four different path lengths.

interface. A wave which is reflected from one interface travels towards the other interface where it experiences transmission and reflection. In Figure 4, the primary wave traveling in +y direction is reflected at the film-cover interface to create a reflected wave (1) traveling in -y direction. This reflected wave (1) is reflected once more at the substrate-film interface to create a reflected wave (3) traveling in +y direction . In the same manner, a principal wave traveling in -y direction is reflected at the substrate-film interface; the result is a reflected wave (2) traveling in +y direction which is in turn reflected at the cover-film interface creating a reflected wave (4) traveling in -y direction. The y dependence of the reflected wave may be correctly determined by the use of a physical picture. Consider the different situations shown in Figure 4. It is seen that there are four principal ways in which a wave traveling from a source point at y' may arrive, via reflection, at the observation point at y. From Figure 4, one can recover the y dependence of the reflected Green's function by determining the four distinct phase path lengths. In fact, the reflected Green's function is comprised of four terms with phases associated with these distinct path lengths. Using Figure 4, the different phase path lengths are: (a) $-y-y'$; (b) $y+y'+2t$; (c) $y-y'+2t$; and (d) $-y+y'+2t$.

2.4 SUMMARY

In a tri-layered dielectric environment, The Hertzian potential Π_x in a current carrying region decomposes into principal and reflected components. The principal wave is that wave which propagates directly from the source to the observation point. Surface polarization currents, which are induced at boundaries of adjacent regions by the primary wave, account for the reflected part.

Integral representations for Π_x may be expressed in either spectral form as

$$\Pi_{xi}(y,z) = \frac{1}{2\pi}\int_{-\infty}^{+\infty} d\zeta \iint_{LCS} \frac{J_x(y',z')}{j\omega\varepsilon_i}\left[g_i^p(y|y';\zeta) + g_i^r(y|y';\zeta) \right] e^{j\zeta(z-z')} dy'dz'$$

or in more standard form as

$$\Pi_{xi}(y,z) = \iint_{LCS} \frac{J_x(y',z')}{j\omega\varepsilon_i} G_i(y|y';z-z')\, dy'dz'$$

where $G_i = G_i^p + G_i^r$ and LCS designates the longitudinal cross section of the dielectric layer where the current is immersed.

The electric field corresponding to the Hertzian potential is given by $E_{xi} = k_i^2\Pi_{xi}$, where i = cover or film. Hence the electric field can be written in terms of the spatial domain Hertz potential Green's function as

$$E_{xi}(y,z) = k_i^2 \iint_{-\infty}^{+\infty} \frac{J_x(y',z')}{j\omega\varepsilon_i} G_i(y|y';z-z')\, dy'dz'$$

We define an electric Green's function $G_i^e(y|y';z-z')$ such that

$$E_{xi}(y,z) = \iint_{-\infty}^{\infty} J_x(y',z')\, G_i^e(y/y';z-z')\, dy'dz' \qquad (2.25)$$

Hence the electric Green's function G^e is defined in terms of the

Hertz potential Green's function G as follows

$$G_i^e(y|y';z-z') = -jk_o Z_o \; G_i(y|y';z-z') \tag{2.26}$$

where k_o and Z_o are the free space wavenumber and intrinsic impedance, respectively.

Chapter Three

TE PROPAGATION MODE SPECTRUM OF ASYMMETRIC PLANAR WAVEGUIDE

3.1 INTRODUCTION

Performing the inverse Fourier transform in eqn(2.20) (eqn(2.24)) leads to the identification of the propagation mode spectrum of asymmetric planar dielectric waveguides (Figure 1), with sources immersed in the film region (in the cover region). Complex ζ-plane analysis facilitates this identification. Use of Cauchy's theorem for contour integrals [10] allows the original real line contour of the inversion integral on the transform domain Green's function to be deformed. An appropriate choice of contour deformation reveals that the field decomposes into two types of modes.

To apply Cauchy's theorem, we must identify the location of singularities of the transform domain Green's function in the complex ζ-plane implicated by the inversion integral for $G(y|y';z-z')$. Existing singularities in the ζ-plane occur near the real ζ-axis at the location of surface-wave poles and at the branch points with associated branch cuts.

Complex plane analysis applied to the spectral integral representation of the Green's function for the sources immersed in the film region will be detailed, whereas the final results will be stated for the case of sources immersed in cover region.

3.2 COMPLEX ζ-PLANE ANALYSIS

Recall the expression for the space domain Hertzian potential Green's function for sources immersed in the film region

$$G(y|y';z-z') = \frac{1}{2\pi}\int_{-\infty}^{+\infty} g(y|y';\zeta)e^{j\zeta(z-z')}d\zeta \tag{3.1}$$

where

$$g(y|y';\zeta) = \frac{1}{2p_f}\Big[e^{-p_f|y-y'|} + R_+^{(1)}\, e^{-p_f(y+y'+2t)}$$
$$+ R_+^{(2)}e^{-p_f(y-y'+2t)} + R_-^{(1)}e^{p_f(y-y'-2t)} + R_-^{(2)}e^{p_f(y+y')}\Big] \tag{3.2}$$

Deformation of this real line integration requires knowledge of the singularities of the integrand in the complex ζ-plane. After locating these singularities, which consist of surface-wave poles and branch points, a discussion of the appropriate branch cut is given. Finally, Cauchy's theorem for contour integrals is applied to determine the appropriate contour used in identifying the propagation spectrum.

3.2.1 Green's Function ζ-Plane Singularities

The integrand in (3.1) has a complicated functional dependence on the multivalued wave number $p_\ell = \pm\sqrt{\zeta^2-k_\ell^2}$ (ℓ=s,c,f for substrate, cover and film). The correct sign of the square root is chosen to implement the radiation condition for $|y| \longrightarrow \infty$ and ensures the convergence of the integral. Hence, the branch that leads to outward-propagating or attenuated waves must be chosen. This requires that

$$\begin{aligned} \mathrm{Re}\{p_\ell\} &> 0 \\ \mathrm{Im}\{p_\ell\} &> 0 \end{aligned} \tag{3.3}$$

The integrand in (3.1) is a multivalued function of ζ [11] because of the two branches of the function p_ℓ. Hence, to ensure that the integrand is analytic, the complex ζ-plane must be cut by branch lines emanating from branch points and extending to a point at infinity. The branch points occur at $\zeta = \pm k_\ell$. Branch points at $\zeta = \pm k_f$ are removable singularities and the branch cuts emanating from them are not implicated, since the integrand in (3.1) is an even function of p_f.

In addition to the branch point singularities, the integrand has a finite number of isolated pole singularities. In fact, the reflection coefficients $R_+^{(1)}$, $R_+^{(2)}$, $R_-^{(1)}$ and $R_-^{(2)}$ have simple poles associated with surface-wave modes supported by the tri-layered environment.

Figure 5 shows the location of the singularities of the integrand in the complex ζ-plane. Real and imaginary parts of ζ are designated ζ_r and ζ_i, respectively. Practical dielectric media exhibit small losses which move the poles and the branch points off the real ζ-axis. It is subsequently assumed that

$$k_\ell = k_{\ell r} + jk_{\ell i} \; ; \qquad k_{\ell r} > 0 \, , \quad k_{\ell i} < 0$$

Hence, all singularities reside in quadrants two and four. At this stage, branch cuts are chosen arbitrarily as long as they do not cross the initial real-line contour C. One possible construction for the branch cut is shown in Figure 5. Subsequent analysis involving contour

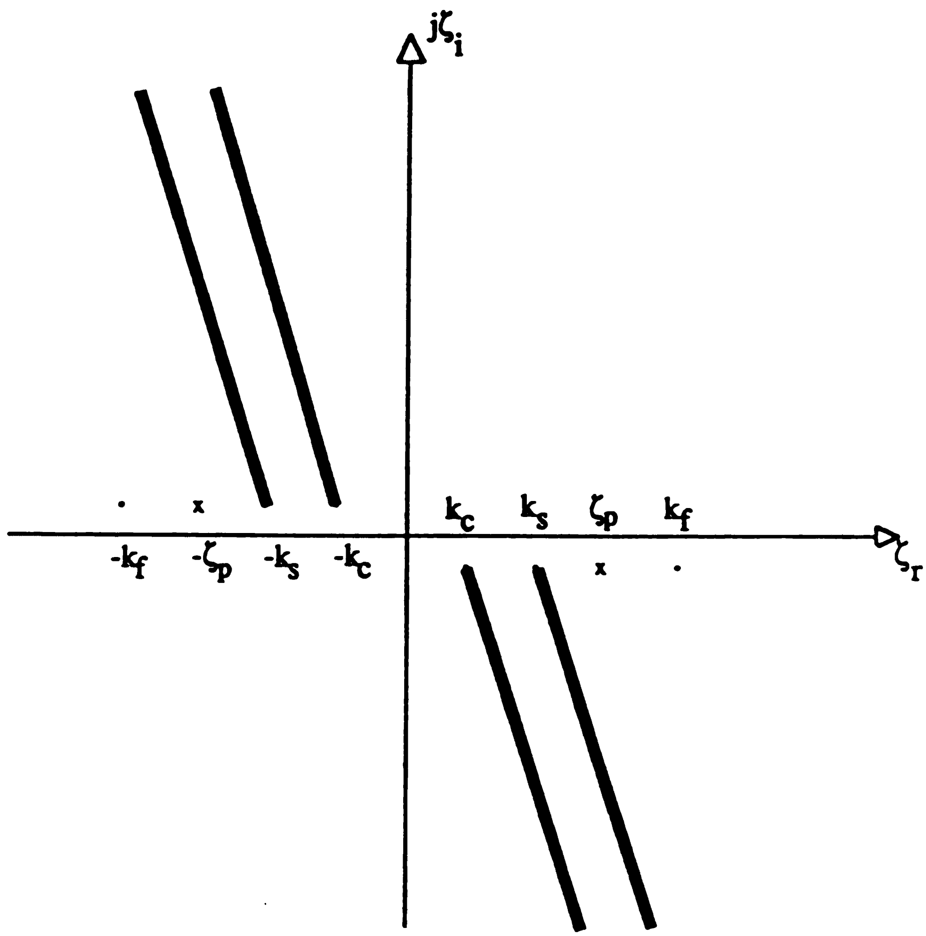

Figure 5: Complex ζ-plane singularities of the transform domain Green's function with arbitrary branch cuts.

deformation demands a particular choice for the branch cuts.

3.2.2 Contour Deformation

Cauchy's theorem provides a powerful analytic technique for evaluating certain types of definite integrals. Specifically, Cauchy's theorem for contour integrals [10] may be used subsequent to deforming the initial real line path for inversion integrals.

Consider for now an arbitrary closed contour C′ in the complex ζ-plane. The correct contour is determined by considering several constraints. First, the branches for each p_ℓ must be chosen so that the integrand of (3.1) represents decaying and outward-propagating waves. As far as the contour C′ is concerned, the branch cuts may be chosen quite arbitrarily as long as they do not intersect the contour C′. Second, it must be decided in which half-plane the contour C′ is to be closed. Therefore, as C is deformed into C′ we have

$$G(y|y';z-z') = \frac{1}{2\pi}\int_{C'} g(y|y';\zeta)e^{j\zeta(z-z')}d\zeta \tag{3.4}$$

As was stated earlier, the radiation conditions are satisfied when $Re\{p_\ell\} > 0$ and $Im\{p_\ell\} > 0$. Writing $p_\ell = \pm\sqrt{\zeta-k_\ell}\,\sqrt{\zeta+k_\ell}$, then for any point ζ along the real ζ-axis, the phase angle of the two factors $(\zeta-k_\ell)$ and $(\zeta+k_\ell)$ lies in the range

$$0 < \arg(\zeta-k_\ell) = \theta_\ell^+ < \pi$$
$$-\pi < \arg(\zeta+k_\ell) = \theta_\ell^- < 0$$

as ζ_r ranges from $-\infty$ to $+\infty$. Those angles were determined from Figure 6.

A careful examination shows that the sum of these arguments satisfies $0 < \theta_\ell^+ + \theta_\ell^- < \pi$. Hence the phase angle of $+\sqrt{\zeta^2-k_\ell^2}$ is always greater than zero but less than $\frac{\pi}{2}$. In order to satisfy the specific requirements on p_ℓ as in eqn (3.3), the positive root or branch must be chosen. Hence

$$p_\ell = +\sqrt{\zeta^2-k_\ell^2} \qquad (3.5)$$

With this branch, the convergence of the integral (3.4) at infinity is ensured.

Secondly, the exponential factor $e^{j\zeta(z-z')}$ appears as part of the integrand in (3.4). Writing $\zeta = \zeta_r+j\zeta_i$ the above exponential factor will be

$$e^{j\zeta(z-z')} = e^{-\zeta_i(z-z')}e^{j\zeta_r(z-z')}$$

Therefore, in the upper half ζ-plane (lower half ζ-plane) this exponential is decaying for $z-z' > 0$ ($z-z' < 0$) while it increases exponentially for $z-z' < 0$ ($z-z' > 0$). Hence, when $z>z'$ ($z<z'$), the contour C must be closed in the upper half ζ-plane (lower half ζ-plane). The correct contour for evaluating (3.4) is thus the one illustrated in Figure 7 such that $C' = C + C_\infty + C_b\pm$.

For $z>z'$, the contour must be closed in the upper half ζ-plane. Since the branch cut cannot be crossed, the contour C′ must come back in from infinity on one side of the branch cut, encircle the branch point at $\zeta = -k_\ell$, and recede out to infinity again along the opposite side of the cut. This contour is illustrated in Figure 7 (dashed) and denoted by C_∞ for the semicircle at infinity and by $C_b^\pm$ for the branch cut integral.

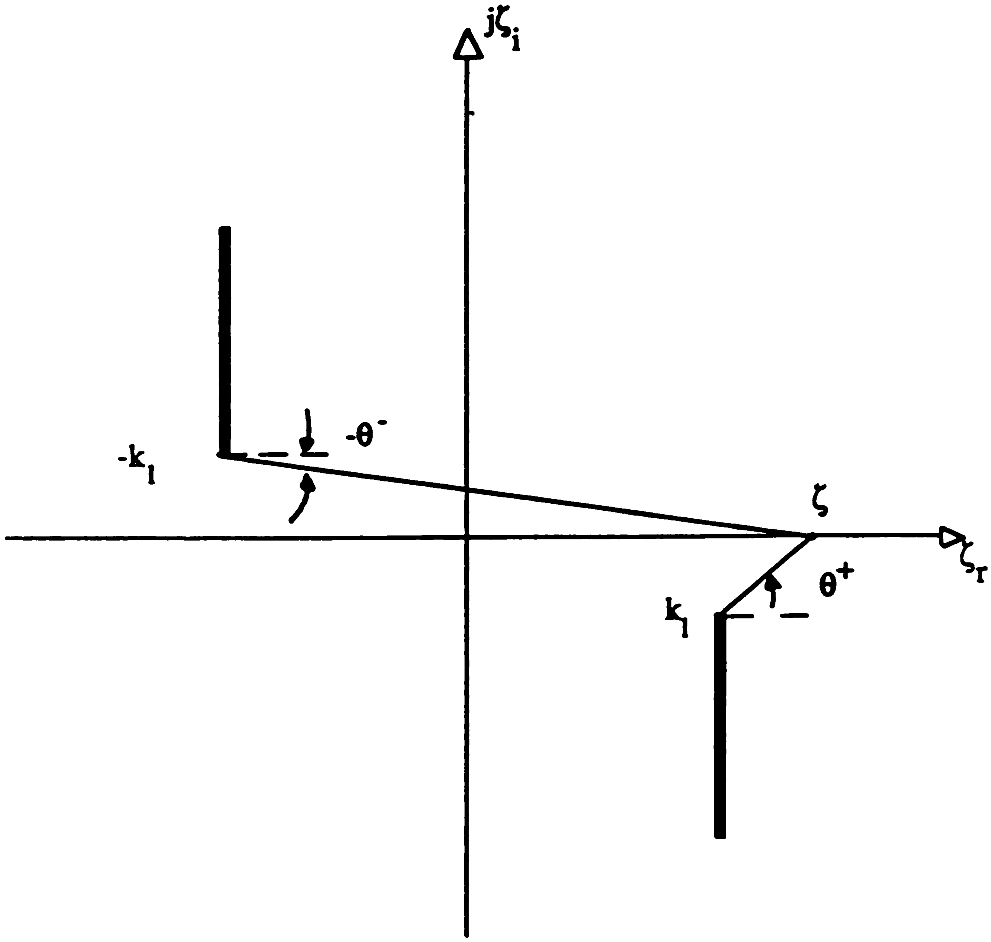

Figure 6: Determination of the proper branch of each p_ℓ.

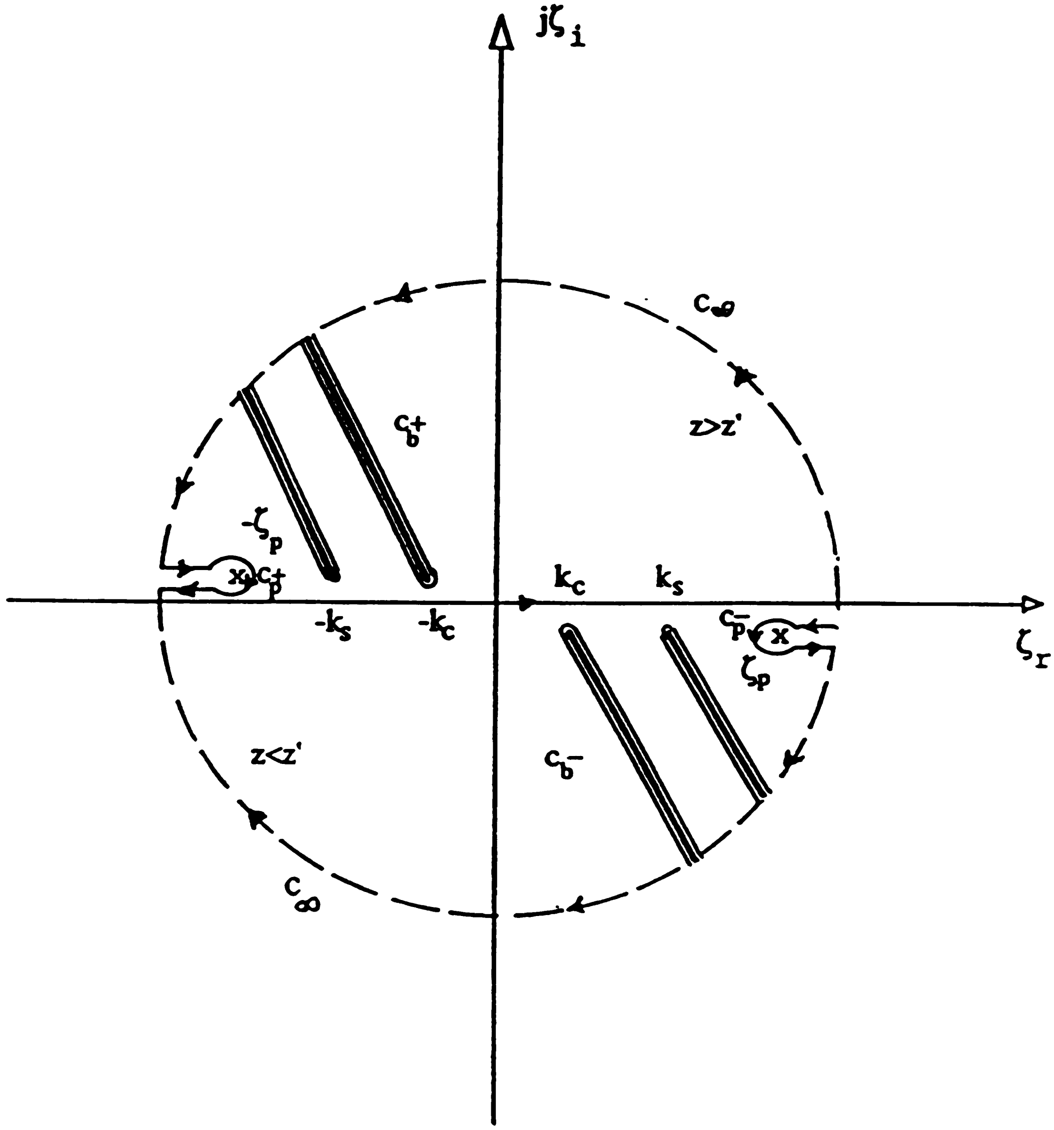

Figure 7: Deformation contour C′ on which the transform domain Green's function is analytic.

Since a branch cut was introduced, the integrand in (3.4) is single valued and Cauchy's theorem applies [11]. Moreover, by deforming the closed contour $C' = C + C_\infty + C_b^\pm$ around the surface wave poles ($\pm\zeta_p$), the integrand in (3.4) will be analytic and Cauchy's theorem for contour integrals leads to

$$\int_{C'} g(y|y';\zeta)e^{j\zeta(z-z')}d\zeta = 0$$

Note that the closed contour C' contains the contour around the surface-wave pole $C_p^\pm$ such that

$$C' = C + C_\infty + C_b^\pm + C_p^\pm$$

where the plus (minus) sign in $C_b^\pm$ and $C_p^\pm$ refers to the contour being in the upper half plane (lower half-plane). The original integration along C is thus replaced by

$$\int_C (\cdot\cdot\cdot\cdot) = -\int_{C_\infty}(\cdot\cdot\cdot\cdot) - \int_{C_b^\pm}(\cdot\cdot\cdot\cdot) - \int_{C_p^\pm}(\cdot\cdot\cdot\cdot) \qquad (3.6)$$

If the integral along the semicircle C_∞ in (3.6) vanishes, then the original integral is equal to the branch cut integral plus the surface-wave pole integral. Hence the space domain Green's function as given by (3.1) may be expressed as

$$G(y|y';z-z') = \frac{1}{2\pi}\left\{-\int_{C_b^\pm} g(y|y';\zeta)e^{j\zeta(z-z')}d\zeta - \int_{C_p^\pm} g(y|y';\zeta)e^{j\zeta(z-z')}d\zeta\right\} \tag{3.6.a}$$

The integrand of $G(y|y';z-z')$ is an even function of ζ except for proportionality to $e^{j\zeta(z-z')}$, hence the lower half-plane closure can be combined with the upper half-plane closure. In fact, since we have performed an upper half-plane closure for $z>z'$ and a lower half-plane closure for $z<z'$, the term $e^{j\zeta(z-z')}$ can be replaced by $e^{j|z-z'|}$. By consequence, with the above change, performing the integration in the upper half-plane is sufficient since it combines both cases where $z>z'$(upper half-plane) and $z<z'$ (lower half-plane) into one. Hence (3.6a) becomes

$$G(y|y';z-z') = \frac{1}{2\pi}\left\{-\int_{C_b^+} g(y|y';\zeta)e^{j\zeta|z-z'|}\,d\zeta - \int_{C_p^+} g(y|y;\zeta')e^{j\zeta|z-z'|}\,d\zeta\right\} \tag{3.7}$$

It is now apparent that the Green's function decomposes into the sum of two fundamentally different spectral contributions. By consequence, the electric Hertz potential and the electric field have the same decomposition. The branch cut integral represents the continuous radiation spectrum, while the pole integral represents the discrete surface-wave modes.

The branch cut must be chosen more carefully now if the integral along C_∞ is to vanish. It can be seen that for $\zeta \in C_\infty$, $g(y|y';\zeta)$ decreases exponentially for $\mathrm{Re}\{p_\ell\} > 0$. It was shown earlier that $e^{j\zeta(z-z')}$ vanishes at C_∞ by choosing the correct half-plane closure. Hence, at C_∞ the integrand in (3.4) vanishes provided $\mathrm{Re}\{p_\ell\} > 0$. In order to ensure that C_∞ remains on the proper branch for which $\mathrm{Re}\{p_\ell\} > 0$, the branch cut emanating from branch point $\pm k_\ell$ has to separate the proper branch of p_ℓ for which $p_{\ell r} > 0$ from the improper branch for which $p_{\ell r} < 0$. The correct branch cut lies along the boundary line between $p_{\ell r} > 0$ and $p_{\ell r} < 0$ and is defined by the line leading to $\mathrm{Re}\{p_\ell\} = 0$ or $|\arg(p_\ell)| = \frac{\pi}{2}$.

Observe that when p_ℓ satisfies $|\arg(p_\ell)| = \frac{\pi}{2}$, p_ℓ^2 satisfies $\arg(p_\ell^2) = \pi$ or (i) $\mathrm{Im}(p_\ell^2) = 0$ and (ii) $\mathrm{Re}\{p_\ell^2\} < 0$. Writing $k_\ell = k_{\ell r} + jk_{\ell i}$, p_ℓ^2 may be written as

$$p_\ell^2 = (\zeta_r^2 - \zeta_i^2) - (k_{\ell r}^2 - k_{\ell i}^2) + j2(\zeta_r\zeta_i - k_{\ell r}k_{\ell i})$$

from which it can be seen that condition (i) is satisfied if and only if

$$\zeta_i = \frac{k_{\ell r}k_{\ell i}}{\zeta_r} \tag{3.8}$$

which defines a pair of hyperbolas. Along the hyperbolas defined by (3.8) we have

$$\mathrm{Re}\{p_\ell^2\} = \frac{(\zeta_r^2 - k_{\ell r}^2)(\zeta_r^2 + k_{\ell i}^2)}{\zeta_r^2}$$

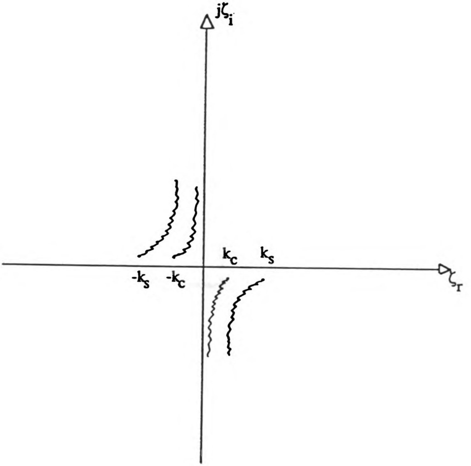

Figure 8: Hyperbolic branch cuts.

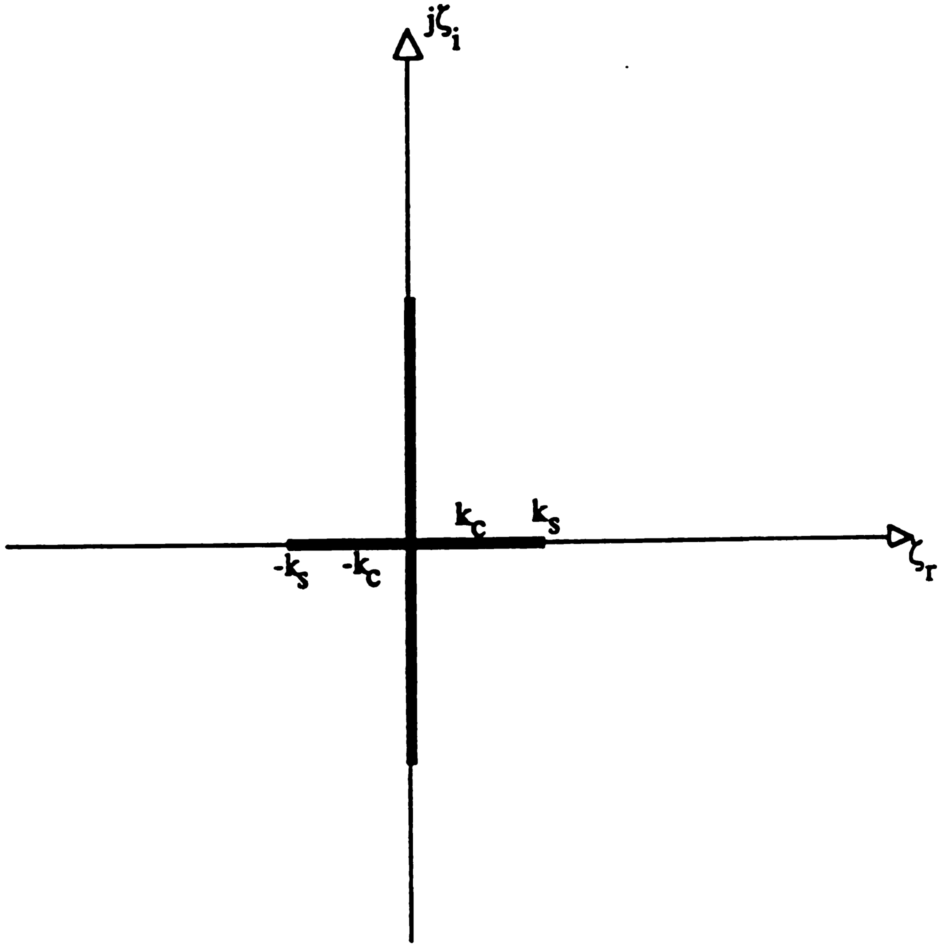

Figure 9: Coalesced branch cut.

In order to satisfy condition (ii), ζ_r must satisfy the inequality

$$-k_{\ell r} < \zeta_r < k_{\ell r} \tag{3.9}$$

Conditions (3.8) and (3.9) describe the portions of the hyperbolas shown in Figure 8. A decrease in the losses associated with the cover and substrate implies a decrease in k_{ci} and k_{si}. In the limit of zero loss, the branch cut emanating from $\pm k_s$ cancels with part of the branch cut emanating from $\pm k_c$ resulting in the cut depicted in Figure 9. In either case of moderate loss or limitingly low loss, these branch cuts guarantee that for all $\zeta \in C_\infty$, $\mathrm{Re}\{p_\ell\} > 0$ and hence the integration along C_∞ vanishes. Thus the validity of (3.7) is ensured.

Now that we have determined the right contour deformation, we proceed with the analysis of the discrete and continuous spectrum.

3.3 THE DISCRETE SPECTRUM

A discrete surface wave mode has been shown to arise from evaluation of the pole integral in the complex ζ-plane. The integrand in (3.4) has poles whenever the reflection coefficients $R_+^{(1)}, R_+^{(2)}$, $R_-^{(1)}$ and $R_-^{(2)}$ become infinite. First, identification of those poles will be performed and then evaluation of the pole integral is presented. We let G_{pole} denote the discrete part of the Green's function in equation (3.7) , then we have

$$G_{pole}(y|y';z-z') = -\int_{C_p^+} \frac{1}{4\pi p_f} \left[R_+^{(1)} e^{-p_f(y+y'+2t)} + R_+^{(2)} e^{-p_f(y-y'+2t)} \right.$$

$$\left. + R_-^{(1)} e^{p_f(y-y'-2t)} + R_-^{(2)} e^{p_f(y+y')} \right] e^{j\zeta|z-z'|} \, d\zeta \tag{3.10}$$

Note that we are integrating around the pole in the upper half plane, that is around $\zeta = -\zeta_p$.

3.3.1 TE Surface Wave-Poles

Recall the expressions for the reflection coefficients $R_+^{(1)}$, $R_+^{(2)}$, $R_-^{(1)}$, $R_-^{(2)}$ from Chapter Two

$$R_+^{(1)} = \frac{(p_f + p_c)(p_f - p_s)\, e^{p_f t}}{2\cosh(p_f t)\left[(p_f^2 + p_c p_s)\tanh(p_f t) + p_f(p_s + p_c)\right]} \tag{3.11a}$$

$$R_+^{(2)} = \frac{(p_f - p_s)(p_f - p_c)\, e^{p_f t}}{2\cosh(p_f t)\left[(p_f^2 + p_c p_s)\tanh(p_f t) + p_f(p_s + p_c)\right]} \tag{3.11b}$$

$$R_-^{(1)} = R_+^{(2)} \tag{3.11c}$$

$$R_-^{(2)} = \frac{(p_f + p_s)(p_f - p_c)\, e^{p_f t}}{2\cosh(p_f t)\left[(p_f^2 + p_c p_s)\tanh(p_f t) + p_f(p_s + p_c)\right]} \tag{3.11d}$$

Note that all the reflection coefficients have the same denominator and hence they are associated with the same simple poles. $R_+^{(1)}$ becomes infinite when

$$Z(\zeta) = (p_f^2 + p_c p_s)\tanh(p_f t) + p_f(p_s + p_c) = 0 \tag{3.12}$$

which leads to TE surface-wave poles at $\zeta = \pm\zeta_p$. We define the following parameters

$$p_f = \sqrt{\zeta^2 - k_f^2} = j\sqrt{k_f^2 - \zeta^2} = jK \tag{3.12a}$$

$$p_c = \sqrt{\zeta^2 - k_c^2} = \gamma \tag{3.12b}$$

$$p_s = \sqrt{\zeta^2 - k_s^2} = \delta \tag{3.12c}$$

The condition that γ of (3.12b) as well as K of (3.12a) are both real quantities limits the range of ζ to the following interval [6]

$$k_c < k_s < \zeta_p < k_f$$

which identifies the region that discrete values of the propagation constant for guided modes can occupy. Using (3.12a) through (3.12c), $Z(\zeta)$ becomes

$$j(\gamma\delta - K^2)\tan Kt = -jK(\gamma + \delta)$$

Rearranging leads to the well-known eigenvalue equation for TE modes of the asymmetric slab

$$\tan Kt = \frac{K(\gamma+\delta)}{K^2 - \gamma\delta} \tag{3.13}$$

We now proceed to evaluate the pole integral in eqn(3.10)

3.3.2 Pole Integral Evaluation

The function of ζ that leads to TE surface-wave poles at $\zeta = \pm\zeta_p$ of eqn(3.12) can be approximated by a Taylor's series of first degree near $\zeta = \pm\zeta_p$. Hence we can write

$$Z(\zeta) \cong Z(\pm\zeta_p) + \left.\frac{dZ}{d\zeta}\right|_{\zeta=\pm\zeta_p} (\zeta\mp\zeta_p)$$

since $Z(\pm\zeta_p)$ vanishes, $Z(\zeta)$ reduces to

$$Z(\zeta) \cong Z'(\pm\,\zeta_p)\ (\zeta\mp\zeta_p) \tag{3.14}$$

where Z' denotes the derivative of $Z(\zeta)$ with respect to ζ.

Rewriting the reflection coefficients $R_+^{(1)}$, $R_+^{(2)}$, $R_-^{(1)}$ and $R_-^{(2)}$ in equations (3.11a) through (3.11d) as follows

$$R_+^{(1)} = \frac{A_1(\zeta)}{Z(\zeta)}\, e^{p_f t}$$

$$R_+^{(2)} = \frac{A_2(\zeta)}{Z(\zeta)}\, e^{p_f t} = R_-^{(1)}$$

$$R_-^{(2)} = \frac{A_3(\zeta)}{Z(\zeta)}\, e^{p_f t}$$

the discrete part of the Green's function in (3.10) becomes

$$G_{pole}(y|y';z-z') = -\int_{C_p^+} \frac{d\zeta}{4\pi p_f Z(\zeta)} \Big[A_1(\zeta)e^{-p_f(y+y'+t)} + A_2(\zeta)e^{-p_f(y-y'+t)}$$

$$+ A_2(\zeta)e^{p_f(y-y'-t)} + A_3(\zeta)e^{p_f(y+y'+t)}\Big] \; e^{j\zeta|z-z'|} \tag{3.15}$$

Making use of the approximation for $Z(\zeta)$ in eqn(3.14), integrating the first term of G_{pole} around the upper half plane surface-wave pole leads to

$$- \int_{C_p^+} \frac{A_1(\zeta)}{4\pi p_f Z'(-\zeta_p)(\zeta+\zeta_p)} \; e^{-p_f(y+y'+t)} \; e^{j\zeta|z-z'|} \; d\zeta$$

$$= \frac{-A_1(\zeta_p)}{4\pi p_f Z'(-\zeta_p)} \; e^{-p_f(\zeta_p)(y+y'+t)} \; e^{-j\zeta_p|z-z'|} \int_{C_p^+} \frac{d\zeta}{\zeta+\zeta_p} \tag{3.16}$$

The integral $\int_{C_p^+} \frac{d\zeta}{\zeta+\zeta_p}$ is evaluated in Appendix D and found to be

$$\int_{C_p^+} \frac{d\zeta}{\zeta+\zeta_p} = -2\pi j$$

the minus sign in front of $2\pi j$ is related to the contour around $\zeta = -\zeta_p$ being directed in the clockwise direction. Hence equation (3.16) becomes

$$- \int_{C_p^+} \frac{A_1(\zeta)}{4\pi p_f Z'(-\zeta_p)(\zeta+\zeta_p)} e^{-p_f(y+y'+t)} e^{-j\zeta_p|z-z'|} d\zeta$$

$$= B_1(\zeta_p) e^{-p_f(\zeta_p)(y+y'+t)} e^{-j\zeta_p|z-z'|}$$

where $B_1(\zeta_p)$ is the amplitude of surface-wave mode contribution from $R_+^{(1)}$ and is expressed as

$$B_1(\zeta_p) = \frac{jA_1(\zeta_p)}{2p_f(\zeta_p)Z'(-\zeta_p)}$$

In the same fashion, the amplitudes of surface-wave mode contributions from $R_+^{(2)}$, $R_-^{(1)}$ and $R_-^{(2)}$ are established as follows

$$B_2(\zeta_p) = \frac{jA_2(\zeta_p)}{2p_f(\zeta_p)Z'(-\zeta_p)}$$

$$B_3(\zeta_p) = \frac{jA_3(\zeta_p)}{2p_f(\zeta_p)Z'(-\zeta_p)}$$

Hence, G_{pole} can be written as

$$G_{pole} = \Big\{ B_1(\zeta_p) e^{-p_f(\zeta_p)(y+y'+t)} + B_2(\zeta_p) e^{-p_f(\zeta_p)(y-y'+t)} + B_2(\zeta_p) e^{p_f(\zeta_p)(y-y'-t)} + B_3(\zeta_p) e^{p_f(\zeta_p)(y+y'+t)} \Big\} e^{-j\zeta_p|z-z'|} \tag{3.17}$$

which expresses the final form for the discrete Green's function.

Now, we have to evaluate each term $A_1(\zeta_p)$, $A_2(\zeta_p)$ and $A_3(\zeta_p)$ as rational functions of p_f, p_c and p_s. The derivative of $Z(\zeta)$ with respect to ζ evaluated at $\zeta = -\zeta_p$ has to be established as well. Using equation (3.12) for $\tanh(p_f t)$, the expression for $\cosh(p_f t)$ can be evaluated from the following

$$\cosh(p_f t) = \frac{1}{\sqrt{1-\tanh^2(p_f t)}}$$

This leads to the expression of $A_1(\zeta_p)$ as a rational function of p_f, p_c and p_s as follows

$$A_1(\zeta_p) = \frac{-\left(p_f^2 + p_f(p_c - p_s) - p_c p_s\right)\sqrt{(k_f^2-k_s^2)(k_f^2-k_c^2)}}{2(p_c p_s + p_f^2)}$$

The coefficients $A_2(\zeta_p)$ and $A_3(\zeta_p)$ are evaluated in the same fashion.

Recalling the expression for $Z(\zeta)$ from equation (3.12), the derivative of $Z(\zeta)$ with respect to ζ is expressed as

$$Z'(\zeta) = (p_c p_s' + p_c' p_s + 2p_f p_f') \tanh(p_f t) + (p_c p_s + p_f^2) t p_f \tanh'(p_f t)$$
$$+ p_f'(p_c + p_s) + p_f(p_c' + p_s')$$

Noting that $\tanh'(p_f t) = 1-\tanh^2(p_f t)$ and exploiting equation (3.12), the derivative of $Z(\zeta)$ with respect to ζ evaluated at $\zeta = -\zeta_p$ can be written as

$$Z'(-\zeta_p) = \frac{-\zeta_p (k_f^2-k_c^2)(k_f^2-k_s^2)}{p_f(p_c p_s + p_f^2)} \left[\frac{p_c + p_s}{p_c p_s} + t \right]$$

Note that in evaluating $Z'(-\zeta)$ we made use of the fact that $p'_\ell = \frac{\zeta}{p_\ell}$ since $p_\ell^2 = \zeta^2 - k_\ell^2$.

Finally, the amplitudes $B_1(\zeta_p)$ through $B_3(\zeta_p)$ in the expression for G_{pole} (equation 3.17) are now expressed as

$$B_1(\zeta_p) = \frac{+j\left(p_f^2 + p_f(p_c - p_s) - p_c p_s\right) p_c p_s}{4\zeta_p \sqrt{(k_c^2 - k_f^2)(k_s^2 - k_f^2)} \left[p_c + p_s + p_c p_s t\right]}$$

$$B_2(\zeta_p) = \frac{+j\left(p_f^2 - p_f(p_s + p_c) + p_s p_c\right) p_c p_s}{4\zeta_p \sqrt{(k_c^2 - k_f^2)(k_s^2 - k_f^2)} \left[p_c + p_s + p_c p_s t\right]}$$

$$B_3(\zeta_p) = \frac{+j\left(p_f^2 - p_f(p_c - p_s) - p_s p_c\right) p_c p_s}{4\zeta_p \sqrt{(k_c^2 - k_f^2)(k_s^2 - k_f^2)} \left[p_c + p_s + p_c p_s t\right]}$$

The mode spectrum, in addition to having a finite number of surface-wave modes, also possesses a continuum of unguided radiation modes.

3.4 CONTINUOUS SPECTRUM

A continuous mode propagation spectrum has been shown to arise from integration along the hyperbolic branch cuts $C_b^{\pm}$ shown in Figure 8. Let $G_R(y|y';z-z')$ denote the continuous part of the spatial domain Green's function in equation (3.7). An examination of the spatially dependent functions which appear in the integrand of G_R reveals that G_R is a spectral superposition of oscillatory y-dependent waves. Hence, the continuous spectrum represents a radiation spectrum.

Recall the expression for G_R from equation (3.7)

$$G_R(y|y';z-z') = -\int_{C_b^+} \frac{1}{4\pi p_f} \Big[e^{-p_f|y-y'|} + R_+^{(1)} e^{-p_f(y+y'+2t)}$$

$$+R_+^{(2)} e^{-p_f(y-y'+2t)} + R_-^{(1)} e^{p_f(y-y'-2t)} + R_-^{(2)} e^{p_f(y+y')} \Big] e^{j\zeta|z-z'|} d\zeta \tag{3.18}$$

Referring to Figure 10, we can see that C_b^+ denotes the branch cut contour associated with branch points at $\zeta = -k_c$ and $\zeta = -k_s$. The branch cut emanating from the branch point at $\zeta = -k_f$ is not significant since the integrand in (3.18) is an even function of p_f. Moreover, in observing Figure 10(a), we can see that the contour above the branch cut emanating from $\zeta = -k_c$ cancels with part of the contour below the branch cut emanating from $\zeta = -k_s$. Therefore, in the case of low loss limit Figure 10(b), both p_s and p_c change signs in crossing the branch cut where $\zeta > -k_c$, whereas only p_s changes sign in crossing the branch cut lying between $-k_s$ and $-k_c$. In the latter case, p_c has the same sign on both sides of the cut.

The branch cut contour C_b^+ can now be divided to include a real line contour along ζ_r and an imaginary line contour along ζ_i as follows

$$\int_{C_b^+} d\zeta = \int_{-k_s}^{-k_c} d\zeta_r + \int_{-k_c}^{0} d\zeta_r + \int_{0}^{\infty} j d\zeta_i \tag{3.19}$$

First, we have to determine the sign of p_ℓ above and below the branch cut along ζ_r and to the right and to the left of the cut along $j\zeta_i$.

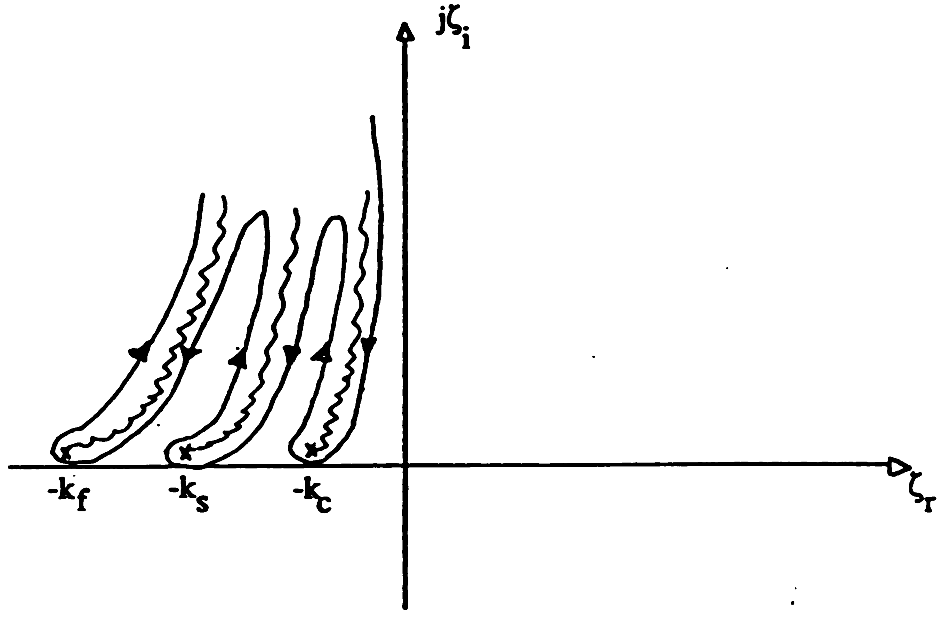

(a) Branch cut contour for the case of some losses

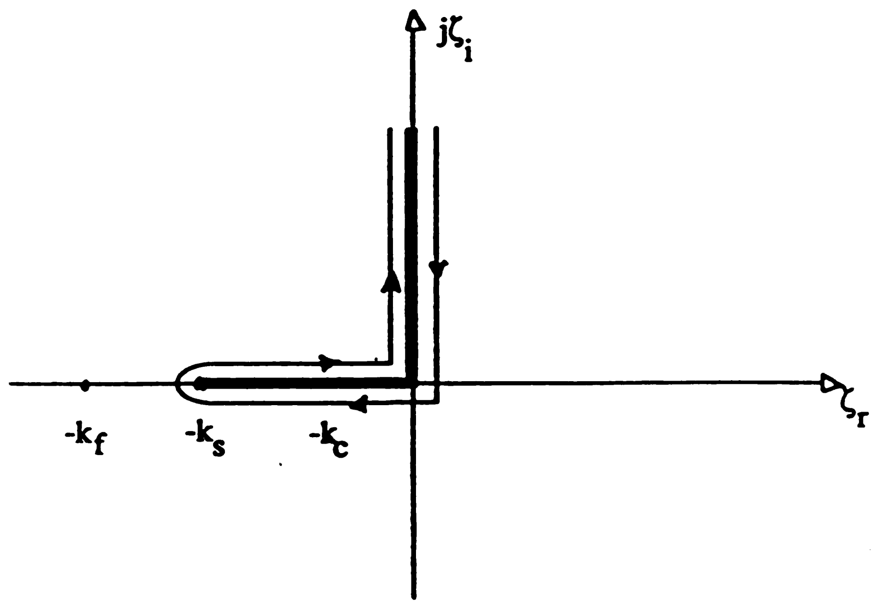

(b) $k_{\ell i} \longrightarrow 0$

Figure 10: Branch cut contour partially cancels for low loss limit.

$p_\ell = \sqrt{\zeta^2 - k_\ell^2}$ can be written as

$$p_\ell = \pm j\sqrt{k_\ell^2-\zeta^2} = \pm j \begin{cases} \sqrt{\zeta_i^2+k_\ell^2} & \text{....along } \zeta_r = 0 \\ \sqrt{k_\ell^2-\zeta_r^2} & \text{....along } \zeta_i = 0 \end{cases}$$

Figure 11 helps in determining the argument of p_ℓ along the branch cut. Along the right and lower sides of the upper half plane branch cut the argument of p_ℓ is equal to $\frac{\pi}{2}$ and hence p_ℓ is positive; along the left and upper sides of the cut, the argument of p_ℓ is equal to $-\frac{\pi}{2}$ showing that p_ℓ is negative there.

Second, we have to determine the behavior of the coefficient $R_+^{(1)}$, $R_+^{(2)}$, $R_-^{(1)}$ and $R_-^{(2)}$ in crossing the branch cut where $\zeta > -k_c$. Along this part of the cut, each of p_ℓ is purely imaginary. Hence, we define the following parameters

$$\left.\begin{aligned} p_c^2 &= \zeta^2 - k_c^2 = -\rho^2 && \text{hence } p_c = j\rho \\ p_s^2 &= \zeta^2 - k_s^2 = -\tau^2 && \text{hence } p_s = j\tau \\ p_f^2 &= \zeta^2 - k_f^2 = -\sigma^2 && \text{hence } p_f = j\sigma \end{aligned}\right\} \tag{3.20}$$

Since the argument of each p_ℓ is $\frac{\pi}{2}$, they are located along the right and lower sides of the upper half plane branch cut ($\zeta > -k_c$).
Exploiting the expression for p_ℓ as in (3.20) in writing the coefficient $R_+^{(1)}$ as in (3.11.a) leads to

$$R_+^{(1)} = \frac{\sigma^2+\sigma(\rho-\tau)-\rho\tau}{2\sigma(\tau+\rho)\cos^2\sigma t + 2(\sigma^2+\rho\tau)\sin^2\sigma t + 2j(\sigma^2+\rho\tau-\sigma(\tau+\rho))\cos\sigma t\sin\sigma t}$$

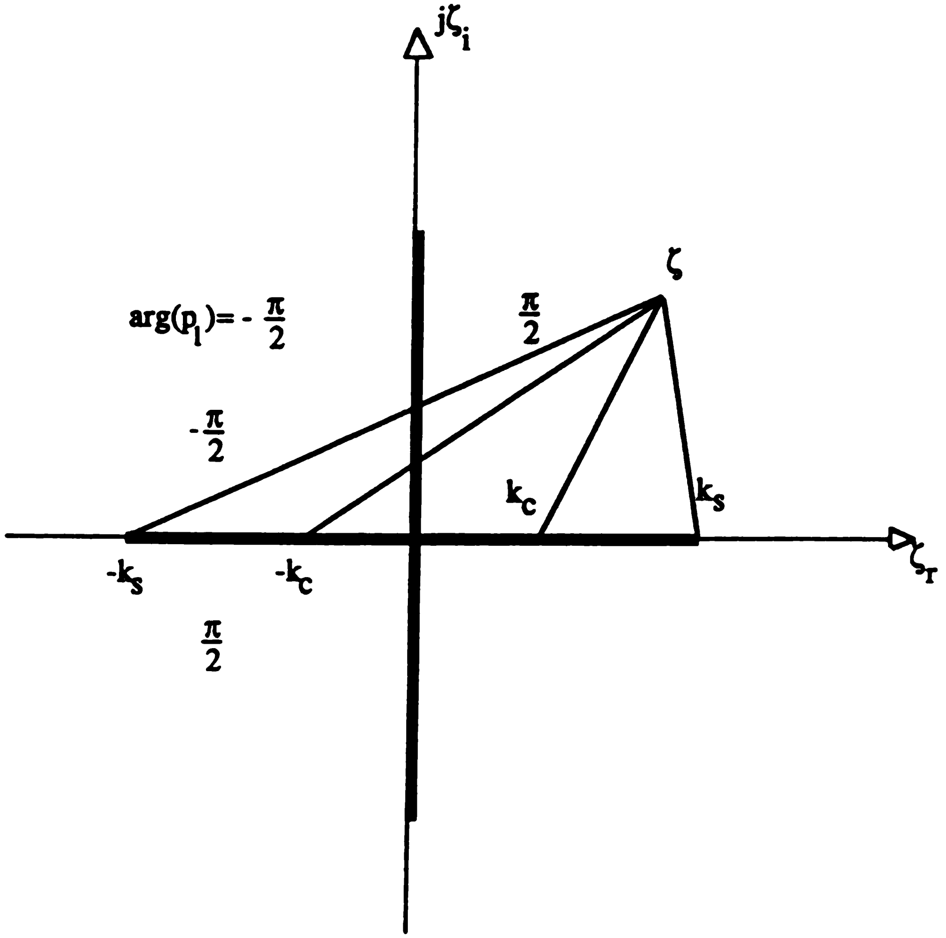

Figure 11: Evaluation of sign of p_ℓ to the left and right of the cut and along upper and lower side of the cut.

which establishes the expression for $R_{+}^{(1)}$ along the right and lower side of the cut. In crossing the branch cut ($\zeta > -k_c$), each p_ℓ will change sign leading to $p_c = -j\rho$, $p_s = -j\tau$ and $p_f = -j\sigma$. Using the form of p_ℓ along the left and upper side of the cut in the expression for $R_{+}^{(1)}$ shows that $R_{+}^{(1)}$ changes to $R_{+}^{(1)*}$ in crossing the branch cut, where the asterisk refers to complex conjugates. In the same fashion , $R_{+}^{(2)}$, $R_{-}^{(1)}$and $R_{-}^{(2)}$ are transformed to their complex conjugate in crossing the branch cut from right to left or from lower to upper side.

Consider now the branch cut lying between $\zeta_r = -k_s$ and $\zeta_r = -k_c$. Along this part of the cut, p_c is real whereas p_s and p_f are purely imaginary and expressed as in (3.20). p_c has the same sign on both sides of the cut. Therefore, p_c is defined as follows

$$p_c^2 = \zeta^2 - k_c^2 = \gamma^2 \qquad\qquad \text{hence } p_c = \gamma = \text{real}$$

The expressions for $R_{+}^{(1)}$, $R_{+}^{(2)}$, $R_{-}^{(1)}$ and $R_{-}^{(2)}$ are changed to their complex conjugates in crossing the lower side of the cut to the upper side. With this in mind, we proceed to evaluate the branch cut integral using (3.19).

As can be seen from equation (3.18) the principal wave component of the radiation Green's function does not depend upon p_s or p_c. Therefore, the only implicated branch cut is that associated with p_f. We have to note that the sum of all the different components of the integrand in G_R is an even function of p_f, whereas each individual component is not. Hence, in integrating along the branch cut contour as in equation (3.19), p_f changes sign (the p_f branch cut is crossed). We choose a convenient sign of p_f since p_c and p_s have constant signs on each different side of the p_f branch cut.

Consequently, we can write the branch cut integral of the principal wave as

$$\int_{C_b^+} \frac{e^{-p_f|y-y'|}}{4\pi p_f} \; e^{j\zeta|z-z'|} \, d\zeta = \int_{-k_s}^{0} (\cdots\cdot) d\zeta_r + \int_{0}^{\infty} (\cdots\cdot) \, j d\zeta_i$$

Note that the integral from $\zeta_r = -k_s$ to $\zeta_r = -k_c$ and the integral from $\zeta_r = -k_c$ to $\zeta_r = 0$ are combined now since the integrand is the same in both regions. Choosing the sign of p_f to be positive along the right and the lower sides of the cut and negative along the left and upper side of the cut, we can write

$$\int_{C_b^+} \frac{e^{-p_f|y-y'|}}{4\pi p_f} \; e^{j\zeta|z-z'|} \, d\zeta$$

$$= \frac{1}{4\pi} \int_{-k_s}^{0} \left[- \frac{e^{-j\sqrt{k_f^2-\zeta_r^2}\;|y-y'|}}{j\sqrt{k_f^2-\zeta_r^2}} + \frac{e^{\;j\sqrt{k_f^2-\zeta_r^2}\;|y-y'|}}{-j\sqrt{k_f^2-\zeta_r^2}} \right] e^{j\zeta|z-z'|} \, d\zeta_r$$

$$+ \frac{1}{4\pi} \int_{0}^{\infty} \left[- \frac{e^{-j\sqrt{k_f^2+\zeta_i^2}\;|y-y'|}}{j\sqrt{k_f^2+\zeta_i^2}} + \frac{e^{j\sqrt{k_f^2+\zeta_i^2}\;|y-y'|}}{-j\sqrt{k_f^2+\zeta_i^2}} \right] e^{-\zeta_i|z-z'|} \, j d\zeta_i$$

(3.21.a)

The first integral has two terms in the integrand because we are considering the lower and upper side of the cut. The minus sign in front of the first integral accounts for the integration being performed in the opposite direction of the branch cut. Now, we want to separate the terms arising from substrate and cover radiation from those arising from substrate radiation only.

After some manipulation equation (3.21.a) becomes

$$\int_{C_b^+} \frac{e^{-p_f|y-y'|}}{4\pi p_f} e^{j\zeta|z-z'|}\, d\zeta$$

$$= \frac{j}{2\pi} \int_{k_s}^{-k_c} \frac{\cos\left(\sqrt{k_f^2-\zeta_r^2}\ |y-y'|\right)}{\sqrt{k_f^2-\zeta_r^2}} e^{j\zeta_r|z-z'|}\, d\zeta_r$$

$$+ \frac{j}{2\pi} \int_{k_c}^{0} \frac{\cos\left(\sqrt{k_f^2-\zeta_r^2}\ |y-y'|\right)}{\sqrt{k_f^2-\zeta_r^2}} e^{j\zeta_r|z-z'|}\, d\zeta_r$$

$$- \frac{1}{2\pi} \int_{0}^{\infty} \frac{\cos\left(\sqrt{k_f^2+\zeta_i^2}\ |y-y'|\right)}{\sqrt{k_f^2+\zeta_i^2}} e^{-\zeta_i|z-z'|}\, d\zeta_i \qquad (3.21b)$$

In the region where $-k_s < \zeta_r < -k_c$, only substrate radiation is present. We define the parameter γ as before where

$$\gamma = \sqrt{\zeta_r^2-k_c^2} \qquad (3.22)$$

and by convention γ is a positive real quantity. From this we can write ζ_r along the negative real axis of the upper half plane branch cut as

$$\zeta_r = -\sqrt{k_c^2+\gamma^2}$$

The first integral $\int_{-k_s}^{-k_c} (\cdots)\, d\zeta_r$ can be conveniently rewritten by changing the integration variable to γ. From equation (3.22) $d\zeta_r$ can be written as

$$d\zeta_r = \frac{\gamma}{\zeta_r}\, d\gamma$$

Also, from equation (3.22) we can see that when $\zeta_r = -k_s$ and $\zeta_r = -k_c$, γ is equal to $k_o\sqrt{n_s^2-n_c^2}$ and zero, respectively .

Similarly, in the region $\zeta > -k_c$ both substrate and cover radiation are present. We define the parameter ρ as before where

$$\rho^2 = k_c^2-\zeta^2 = \begin{cases} k_c^2-\zeta_r^2 \ldots \text{along} \zeta_i=0 \\ k_c^2+\zeta_i^2 \ldots \text{along} \zeta_r=0 \end{cases} \tag{3.23}$$

The latter two integrals in equation (3.21.b) can be conveniently combined. The integration variables are changed from ζ_r and ζ_i to ρ in both cases. From equation (3.23) when ζ_r is equal to zero and $-k_c$, ρ is equal to k_c and zero respectively. Hence we have

$$\zeta = \begin{cases} -\sqrt{k_c^2-\rho^2} & \ldots\text{for } 0 \le \rho \le k_c \\ j\sqrt{\rho^2-k_c^2} & \ldots\text{for } k_c \le \rho < \infty \end{cases}$$

With all this in mind, rearranging equation (3.21.b) leads to

$$\int_{C_b^+} \frac{e^{-p_f|y-y'|}}{4\pi p_f} e^{j\zeta|z-z'|} \; d\zeta$$

$$= \frac{-j}{2\pi} \left[\int_0^{k_0\sqrt{n_s^2-n_c^2}} \frac{\cos\left(\sigma(\gamma)(y-y')\right)}{\sigma(\gamma)} e^{j\zeta(\gamma)|z-z'|} \frac{\gamma}{\zeta(\gamma)} d\gamma \right.$$

$$\left. + \int_0^{\infty} \frac{\cos\left(\sigma(\rho)(y-y')\right)}{\sigma(\rho)} e^{j\zeta(\rho)|z-z'|} \frac{\rho}{\zeta(\rho)} d\rho \right]$$

where

$$\zeta(\rho) = -\sqrt{\gamma^2+k_c^2} \tag{3.24}$$

in the first integral term and

$$\zeta(\rho) = \begin{cases} -\sqrt{k_c^2-\rho^2} & \ldots.0 \le \rho \le k_c \\ +j\sqrt{\rho^2-k_c^2} & \ldots.k_c \le \rho < \infty \end{cases} \tag{3.25}$$

in the second integral term. Also, since $\sigma^2 = k_f^2-\zeta^2$ we have

$$\sigma = \begin{cases} \sigma(\gamma) = \sqrt{k_0^2(n_f^2-n_c^2)-\gamma^2} & \ldots.\text{first integral} \\ \sigma(\rho) = \sqrt{k_0^2(n_f^2-n_c^2)+\rho^2} & \ldots.\text{second integral} \end{cases} \tag{3.26}$$

The reflected wave component of the radiation Green's function is analyzed in the same fashion as for the principal component, taking into account that the different reflection coefficients are transformed to their complex conjugates as the branch cut is crossed. Hence, G_R can be expressed as

$$
\begin{aligned}
G_R(y|y';z-z') = -\int_{C_b^+}\Bigg[\, & e^{-p_f|y-y'|} + R_+^{(1)}e^{-p_f(y+y'+2t)} \\
& + R_+^{(2)}e^{-p_f(y-y'+2t)} + R_-^{(1)}e^{p_f(y-y'-2t)} + R_-^{(2)}e^{p_f(y+y')}\Bigg]\frac{e^{j\zeta|z-z'|}}{4\pi p_f(\zeta)}\,d\zeta \\
+ \frac{j}{2\pi}\Bigg[\int_0^{k_0\sqrt{n_s^2-n_c^2}} & \Bigg\{\cos\sigma(\gamma)(y-y') + \mathrm{Re}\Big\{R_+^{(1)}\;e^{-j\sigma(\gamma)(y+y'+2t)}\Big\} \\
& + \mathrm{Re}\Big\{R_+^{(2)}\;e^{-j\sigma(\gamma)(y-y'+2t)}\Big\} + \mathrm{Re}\Big\{R_-^{(1)}\;e^{j\sigma(\gamma)(y-y'-2t)}\Big\} \\
& + \mathrm{Re}\Big\{R_-^{(2)}\;e^{j\sigma(\gamma)(y+y')}\Big\}\Bigg\}\,e^{j\zeta(\gamma)|z-z'|}\frac{\gamma\,d\gamma}{\sigma(\gamma)\,\zeta(\gamma)} \\
+ \int_0^{\infty} & \Bigg\{\cos\sigma(\rho)(y-y') + \mathrm{Re}\Big\{R_+^{(1)}e^{-j\sigma(\rho)(y+y'+2t)}\Big\} \\
& + \mathrm{Re}\Big\{R_+^{(2)}\;e^{-j\sigma(\rho)(y-y'+2t)}\Big\} + \mathrm{Re}\Big\{R_-^{(1)}\;e^{j\sigma(\rho)(y-y'-2t)}\Big\} \\
& + \mathrm{Re}\Big\{R_-^{(2)}\;e^{j\sigma(\rho)(y+y')}\Big\}\Bigg\}\,e^{j\zeta(\rho)|z-z'|}\frac{\rho\,d\rho}{\sigma(\rho)\,\zeta(\rho)}\Bigg]
\end{aligned}
\tag{3.27}
$$

which establishes the final form of the space domain Hertz potential radiation Green's function. The parameters $\zeta(\gamma)$, $\zeta(\rho)$, $\sigma(\gamma)$ and $\sigma(\rho)$ are expressed as in equations (3.24) through (3.26).

3.5 COMPLEX PLANE ANALYSIS FOR THE CASE OF SOURCES IMMERSED IN THE COVER

Recall form Chapter Two, the expression of the spectral representation of the Hertz potential Green's function with sources immersed in the cover layer

$$G(y|y';z-z') = \frac{1}{2\pi} \int_{-\infty}^{\infty} \frac{1}{2p_c} \left\{ e^{-p_c|y-y'|} + R(\zeta)\, e^{-p_c(y+y')} \right\} e^{j\zeta(z-z')} d\zeta$$

where the reflection coefficient $R(\zeta)$ is expressed as

$$R(\zeta) = \frac{p_f(p_c-p_s) + (p_c p_s - p_f^2)\tanh(p_f t)}{p_f(p_s+p_c) + (p_s p_c + p_f^2)\tanh(p_f t)}$$

Note that the second term of the spectral integral representation of the Hertz potential Green's function involving $R(\zeta)$ contributes surface wave modes associated with simple poles of $R(\zeta)$. Radiation modes associated with branch cuts of p_c and p_s are contributed by both terms. Branch cuts associated with p_f are not implicated since the integrand of $G(y|y';z-z')$ is an even function of p_f.

Deformation of the real line integration path leads to the same contour C'as when sources were immersed in the film layer (Figure 7). In fact, the radiation condition is the same in both cases. Equating the denominator of $R(\zeta)$ to zero leads to the well known eigenvalue equation for TE modes of the asymmetric slab as in equation (3.13). Evaluating the pole integral in complex ζ-plane gives the discrete part of the Green's function as

$$G_{pole}(y|y';z-z') = B(\zeta_p)\, e^{-p_c(\zeta_p)(y+y')} e^{-j\zeta_p|z-z'|}$$

where

$$B(\zeta_p) = \frac{j p_c p_s p_f^2}{\zeta_p (k_f^2-k_c^2)(p_c+p_s+p_c p_s t)}$$

The evaluation of the branch cut integral is similar to the case of the sources immersed in the film region. $R(\zeta)$ changes to its complex conjugate in crossing the upper half plane branch cut from right to left or from lower to upper side. The expression for the radiation component of the Green's function is then formulated as

$$G_R(y|y';z-z') = \frac{-j}{2\pi}\left[\int_0^{k_0\sqrt{n_s^2-n_c^2}} \mathrm{Im}\left\{R(\zeta)\, e^{-\gamma(y+y')}\right\} \frac{e^{-j\zeta(\gamma)|z-z'|}}{\zeta(\gamma)}\, d\gamma \right.$$

$$\left. - \int_0^{\infty}\left\{\cos\rho(y-y') + \mathrm{Re}\left\{R(\zeta)\, e^{-j\rho(y+y')}\right\}\right\} \frac{e^{-j\zeta(\rho)|z-z'|}}{\zeta(\rho)}\, d\rho\right]$$

where

$$\zeta(\gamma) = \sqrt{\gamma^2+k_c^2} \qquad \text{.....in the first integral term}$$

and

$$\zeta(\rho) = \sqrt{k_c^2-\rho^2} = \begin{cases} \sqrt{k_c^2-\rho^2} & \text{....for } 0 \le \rho \le k_c \\ -j\sqrt{\rho^2-k_c^2} & \text{....for } k_c \le \rho < \infty \end{cases}$$

.....in the second integral term

3.6 SUMMARY

Identification of the propagation mode spectrum of asymmetric planar slab waveguides may be made by analyzing solutions to (2.20) or

(2.24) in the complex ζ-plane. By appropriately deforming the initial real-line inversion integral of the transform domain Green's function, the space domain Green's function may be expressed as

$$G(y|y';z-z') = -\frac{1}{2\pi}\int_{C_p^+} g(y/y';\zeta)\ e^{j\zeta|z-z'|}\ d\zeta$$

$$-\frac{1}{2\pi}\int_{C_b^+} g(y/y';\zeta)\ e^{j\zeta|z-z'|}\ d\zeta$$

where C_p^+ and C_b^+ are the contour around the pole and the hyperbolic branch cut in the upper half plane respectively.

From eqn (2.25) it can be seen that the electric field decomposes into a superposition of two types of modes. A discrete mode spectrum arises from integrating around the surface-wave pole in the complex ζ-plane while spectral components of the continuous spectrum are given by (2.20) or (2.24) along the branch cut contour C_b^+.

$$G_f^e(y|y';z-z') = -jk_oZ_o \left[G_{pole}(y|y';z-z') + G_R(y|y';z-z') \right]$$

$$= -jk_oZ_o \Bigg[\Big\{ B_1(\zeta_p)\, e^{-p_f(\zeta_p)(y+y'+t)} + B_2(\zeta_p)\, e^{-p_f(\zeta_p)(y-y'+t)}$$

$$+ B_2(\zeta_p)\, e^{p_f(\zeta_p)(y-y'-t)} + B_3(\zeta_p)\, e^{p_f(y+y'+t)} \Big\}\, e^{-j\zeta_p|z-z'|}$$

$$+ \frac{j}{2\pi} \Bigg[\int_0^{k_o\sqrt{n_s^2-n_c^2}} \Big\{ \cos\sigma(\gamma)(y-y') + \mathrm{Re}\Big\{ R_+^{(1)}\, e^{-j\sigma(\gamma)(y+y'+2t)} \Big\}$$

$$+ \mathrm{Re}\Big\{ R_+^{(2)}\, e^{-j\sigma(\gamma)(y-y'+2t)} \Big\} + \mathrm{Re}\Big\{ R_+^{(2)}\, e^{j\sigma(\gamma)(y-y'-2t)} \Big\}$$

$$+ \mathrm{Re}\Big\{ R_-^{(2)}\, e^{j\sigma(\gamma)(y+y')} \Big\} \Big\}\, e^{j\zeta(\gamma)|z-z'|}\, \frac{\gamma\, d\gamma}{\sigma(\gamma)\,\zeta(\gamma)}$$

$$+ \int_0^{\infty} \Big\{ \cos\sigma(\rho)(y-y') + \mathrm{Re}\Big\{ R_+^{(1)} e^{-j\sigma(\rho)(y+y'+2t)} \Big\}$$

$$+ \mathrm{Re}\Big\{ R_+^{(2)}\, e^{-j\sigma(\rho)(y-y'+2t)} \Big\} + \mathrm{Re}\Big\{ R_+^{(2)}\, e^{j\sigma(\rho)(y-y'-2t)} \Big\}$$

$$+ \mathrm{Re}\Big\{ R_-^{(2)}\, e^{j\sigma(\rho)(y+y')} \Big\} \Big\}\, e^{j\zeta(\rho)|z-z'|}\, \frac{\rho\, d\rho}{\sigma(\rho)\,\zeta(\rho)} \Bigg]$$

(3.28)

This electric Green's function will be used in next chapter to evaluate the unknown electric field inside a discontinuity in the film region.

Chapter Four

APPLICATION TO SCATTERING BY OBSTACLES ALONG ASYMMETRIC SLAB WAVEGUIDE

4.1 INTRODUCTION

When the geometry of the waveguide is perfect, and if we can neglect losses in the dielectric material itself, the guided modes will travel without change and without attenuation. It is, however, impossible to build dielectric waveguides to such a perfection. Studying the modes of a perfect waveguide as was done in the previous chapters is an important first step of determining its properties. In order to be able to evaluate the performance of a realistic waveguide, it is necessary to study its behavior if departures from the perfect geometry occur.

The imperfections of dielectric waveguides occur in many forms: (1) losses of the dielectric material, (2) departure from perfect straightness, (3) inhomogeneities of the dielectric material, (4) departure of the core/cladding interface from a perfect plane in slab waveguides, and (5) many others. Of all imperfections mentioned, the influence of inhomogeneities of the dielectric material in the core region will be analyzed. Waves scattered by such a discontinuity along the guiding structure can be quantified on the basis of a polarization electric field integral-equation (EFIE) description of the discontinuity field.

Various methods have been presented by several authors for the analysis of discontinuity problems in slab waveguides. Among those is

Marcuse's treatment [12,13] which dealt with the abrupt junction between two dissimilar guides and the interaction of surface waves with small, distributed surface irregularities. The most rigorous analysis for step discontinuities is Rozzi's investigation [1,14] based on a two-dimensional integral equation formulation for the fields in transverse discontinuity planes.

A polarization EFIE description of slice discontinuities along a symmetric-slab waveguide was first exploited by Nyquist and Hsu [2,3]. Subsequent applications of the integral-operator description [4,5] were based on different representations of the Green's function kernel and expansions of the unknown field. The EFIE formulation in [2] and [3] was generalized [6] to include discontinuities having arbitrary shapes and complex refractive index profiles along open boundary dielectric waveguides.

In this chapter, a polarization EFIE description of the discontinuity region along an asymmetric-slab guide is developed. Method of moment (MOM) numerical solutions were obtained for the discontinuity field, leading to scattering coefficients and the fractional radiated power.

4.2 EQUIVALENT-POLARIZATION DESCRIPTION OF DISCONTINUITY REGION

An equivalent polarization description of the dielectric discontinuity region is obtained in terms of the contrast of its refractive index against that of the unperturbed surface waveguide. Figure 12 indicates a dielectric discontinuity along an open-boundary

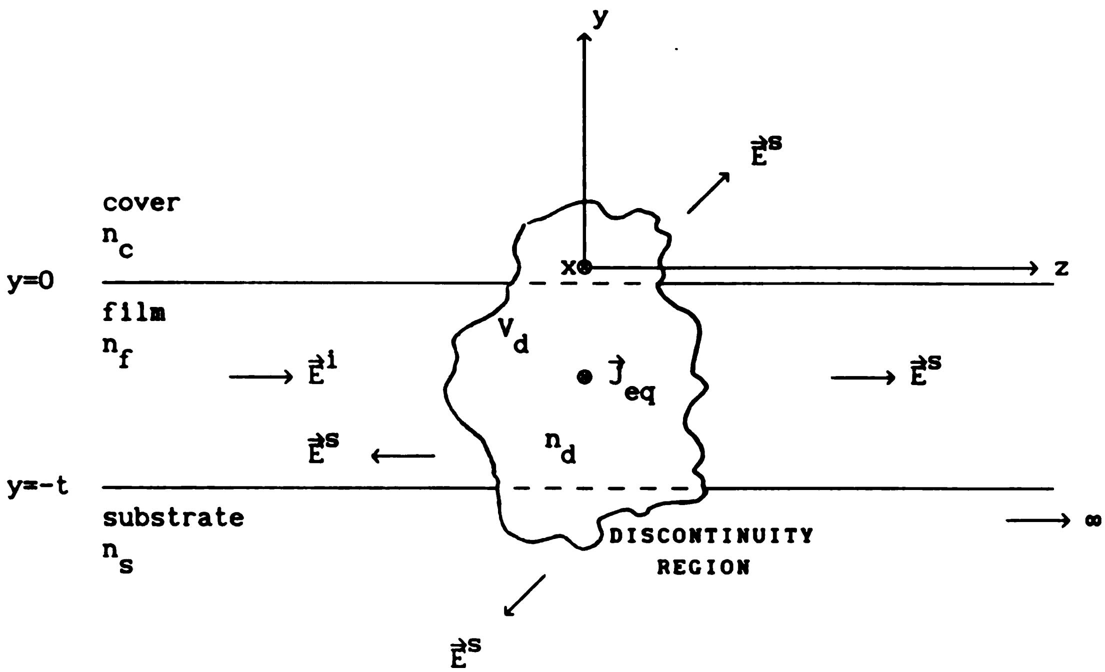

Figure 12: Scattering (reflection, transmission, and radiation) of an incident TE_1 surface-wave mode by a dielectric -slice discontinuity along a planar-slab waveguide of arbitrary shape.

dielectric waveguide. When a surface-wave mode is incident upon the discontinuity, it is subsequently scattered; i.e, it is reflected, transmitted and radiated. Let $n_u(\vec{r})$ denote the refractive index of the unperturbed surface waveguide with the decomposition

$$n_u = \begin{cases} n_s(\vec{r}) & \text{...at points in the substrate} \\ n_f(\vec{r}) & \text{...at points in the waveguide core} \\ n_c(\vec{r}) & \text{...at points in cladding} \end{cases}$$

The discontinuity region V_d with refractive index $n_d(\vec{r})$ is that region where the refractive index differs from $n_u(\vec{r})$. The incident wave $\vec{E}^i$ induces an equivalent polarization distribution in region V_d, and this polarization excites and maintains the scattered field $\vec{E}^s$.

We know from Ampere's law at any point in the system

$$\nabla \times \vec{H}(\vec{r}) = \vec{J}^e(\vec{r}) + j\omega\varepsilon(\vec{r})\,\vec{E}(\vec{r})$$

where $\varepsilon(\vec{r})$ denotes either the unperturbed permittivity $\varepsilon_u(\vec{r})$ in the unperturbed region or $\varepsilon_d(\vec{r}) = n_d^2(\vec{r})\varepsilon_o$ in the discontinuity region. $\vec{J}^e(\vec{r})$ is the impressed electric current which maintains an impressed incident field $\vec{E}^i$. An equivalent polarization current is obtained [15] by adding and subtracting the displacement current of the unperturbed current in the Ampere's law Maxwell equation. We obtain

$$\begin{aligned} \nabla \times \vec{H}(\vec{r}) &= \vec{J}^e(\vec{r}) + j\omega\varepsilon_o(n^2-n_u^2)\,\vec{E}(\vec{r}) + j\omega\varepsilon_o n_u^2\,\vec{E}(\vec{r}) \\ &= \vec{J}^e(\vec{r}) + \vec{J}_{eq}(\vec{r}) + j\omega\varepsilon_o n_u^2\,\vec{E}(\vec{r}) \end{aligned}$$

where

$$\vec{J}_{eq}(\vec{r}) = j\omega\varepsilon_o(n^2-n_u^2)\,\vec{E}(\vec{r})$$

is the equivalent induced polarization current which describes the

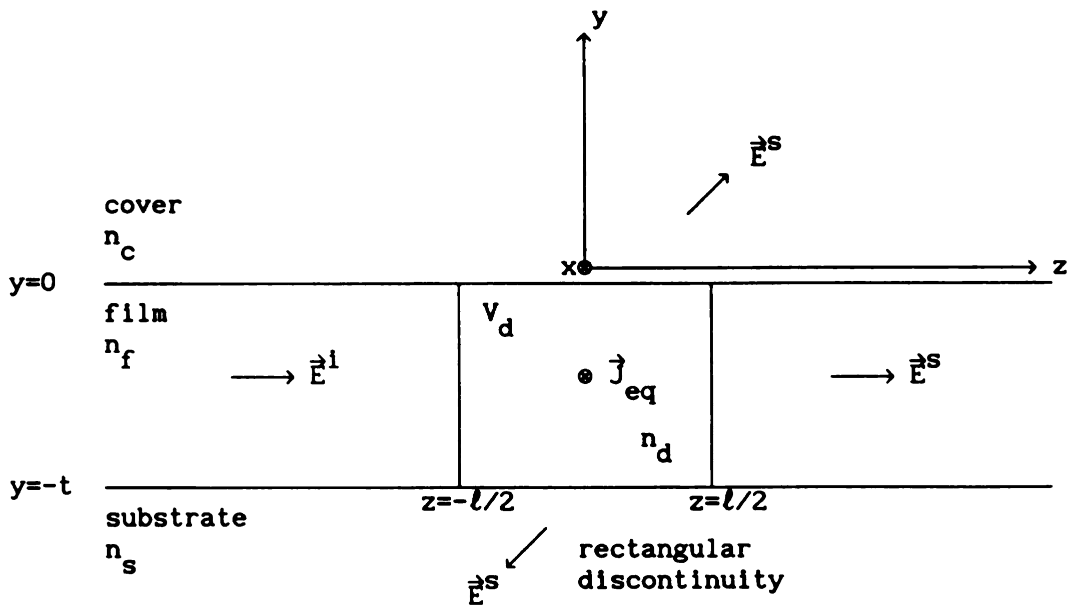

Figure 13: Scattering (reflection, transmission, and radiation) of an incident TE_1 surface-wave mode by a dielectric -slice discontinuity along a planar-slab waveguide of rectangular shape.

discontinuity region V_d and excites the scattered field $\vec{E}^s$. The induced current, non vanishing only in the discontinuity region V_d, is expressed in terms of the total field $\vec{E}(\vec{r})$ in that region as

$$\vec{J}_{eq}(\vec{r}) = j\omega\varepsilon_0 \delta n^2(\vec{r})\ \vec{E}(\vec{r})$$

where $\delta n^2(\vec{r}) = n_d^2(\vec{r}) - n_u^2(\vec{r})$ is the refractive index contrast.

We specialize this result to a rectangular discontinuity placed in the film region as in Figure 13. Since the unperturbed refractive index n_u is now equal to n_f, we have

$$\vec{J}_{eq}\ (\vec{\rho}) = j\omega\varepsilon_0 (n_d^2 - n_f^2)\ \vec{E}(\vec{\rho}) = j\omega\varepsilon_0 \delta n^2(\vec{\rho})\ \vec{E}(\vec{\rho}) \tag{4.1}$$

which expresses the excess current of the discontinuity in the film region and where $\vec{\rho} = \hat{y}y + \hat{z}z$ is the 2-D position vector.

4.3 FIELDS MAINTAINED BY IMPRESSED AND INDUCED CURRENTS

Total electric field $\vec{E}$ along the open-boundary surface waveguide is excited by an effective current $\vec{J} = \vec{J}^e + \vec{J}_{eq}$ consisting of both primary impressed and equivalent induced components. The effective current $\vec{J}$ is oriented in the $\hat{x}$ direction in order to excite TE type modes.

The total field along the perturbed waveguide system can be expressed as

$$E_x(y,z) = \int_{LCS} G_f^e(y|y';z-z')\ J_x(y',z')\ dy'dz'$$

which illustrates the E field maintained by $\vec{J}$ in terms of the electric

Green's function expressed as in chapter three. $G_f^e(y|y';z-z')$ is decomposed into discrete and continuous spectral contributions as follows

$$G_f^e(y|y';z-z') = G_{pole}^e(y|y';z-z') + G_R^e(y|y';z-z') \qquad (4.2)$$

where G_R^e and G_{pole}^e are expressible as in Chapter Three.
Equation (4.2), a representation of the electric Green's function, is constructed from complex analysis on the spectral integral representation of the Hertz potential Green's function. Some of the terms in the expression for G_f^e can be combined to emphasize the reciprocity of the electric Green's function. In fact, $G_f^e(y|y';z-z')$ can be written as

$$G_f^e(y|y';z-z') = -jk_0Z_0\Bigg[\Big\{B_1(\zeta_p)\ e^{-jK(y+y'+t)}+2B_2(\zeta_p)\ \cos K(y-y')e^{-jKt}$$

$$+\ B_3(\zeta_p)\ e^{jK(y+y'+t)}\Big\}\ e^{-j\zeta_p|z-z'|}$$

$$+\ \frac{j}{2\pi}\Bigg[\int_0^{k_0\sqrt{n_s^2-n_c^2}}\Big\{\cos\sigma(\gamma)(y-y')$$

$$+\ \mathrm{Re}\Big\{R_+^{(1)}\ e^{-j\sigma(\gamma)(y+y'+2t)}\Big\}$$

$$+\ 2\mathrm{Re}\Big\{R_+^{(2)}\ e^{-j\sigma(\gamma)(2t)}\cos\sigma(\gamma)(y-y')\Big\}$$

$$+\ \mathrm{Re}\Big\{R_-^{(2)}\ e^{j\sigma(\gamma)(y+y')}\Big\}\Big\}\ e^{j\zeta(\gamma)|z-z'|}\frac{\gamma\ d\gamma}{\sigma(\gamma)\ \zeta(\gamma)}$$

$$+\ \int_0^{\infty}\Big\{\cos\sigma(\rho)(y-y')\ +\ \mathrm{Re}\Big\{R_+^{(1)}e^{-j\sigma(\rho)(y+y'+2t)}\Big\}$$

$$+\ 2\mathrm{Re}\Big\{R_+^{(2)}\ e^{-j\sigma(\rho)(2t)}\cos\sigma(\rho)(y-y')\Big\}$$

$$+\ \mathrm{Re}\Big\{R_-^{(2)}\ e^{j\sigma(\rho)(y+y')}\Big\}\Big\}\ e^{j\zeta(\rho)|z-z'|}\frac{\rho\ d\rho}{\sigma(\rho)\ \zeta(\rho)}\Bigg]\Bigg] \qquad (4.2a)$$

4.4 ELECTRIC FIELD INTEGRAL EQUATION FOR AN UNKNOWN FIELD INDUCED IN THE DISCONTINUITY REGION

The field excited along an open-boundary dielectric waveguide and within the discontinuity region by impressed and induced currents is

$$E_x(y,z) = \int_{LCS} G_f^e(y|y';z-z') \left[J_x^e(y',z') + J_{eq}(y',z')\right] ds'$$

$$= E_x^i(y,z) + E_x^s(y,z) \tag{4.3}$$

which represents the electric field at any point in the system. $E_x^i(y,z)$ is the impressed field maintained by a primary impressed current J_x^e and $E_x^s(y,z)$ is the scattered field maintained by excess polarization current J_{eq} induced in the discontinuity region. Rearranging leads to

$$E_x(y,z) - E_x^s(y,z) = E_x^i(y,z) \qquad \text{for all } (y,z) \in \text{LCS} \tag{4.4}$$

where

$$E_x^s(y,z) = j\omega\varepsilon_0 \int_{LCS} \delta n^2(y',z')\, G_f^e(y|y';z-z')\, E_x(y',z')\, ds' \tag{4.5}$$

is the scattered field maintained by an induced current in the discontinuity region with longitudinal cross section LCS. Expressing E_x^s in equation (4.4) in terms of the total field E_x within the discontinuity region by using equation (4.5) leads to the EFIE

$$E_x(y,z) \quad - j\frac{k_o}{Z_o}\int_{LCS} \delta n^2(y',z')G_f^e(y|y';z-z')E_x(y',z')dy'dz' \; = \; E_x^i(y,z)$$

for all $(y,z) \in$ LCS

(4.6)

where $k_o = \omega(\mu_o\varepsilon_o)^{1/2}$ is the free space wavenumber and $Z_o = (\mu_o\varepsilon_o)^{1/2}$ is the associated intrinsic impedance. It is assumed that J_x^e is a remote source that maintains impressed field E_x^i consisting of a single principal TE surface wave mode in the region of interest.

4.4.1 TE Surface Waves Supported by Planar Layered Background

We assume that the film thickness t in Figure 13 is chosen such as to support only the TE_1 principal surface-wave mode. The basic equations for TE-mode guided waves are [13]

$$\left.\begin{aligned} &\nabla_t^2 h_z + (k_\ell^2-\zeta^2)\, h_z = 0 \\ &\vec{e}_t = \frac{\omega\mu}{\zeta}\,(\hat{z}\times\vec{h}_t) \\ &\vec{h}_t = \frac{j\zeta}{(k_\ell^2-\zeta^2)}\,\nabla_t h_z \end{aligned}\right\} \qquad (4.7)$$

where ℓ = s,f,c (substrate/film/cover) and lower case $\vec{h}$ and $\vec{e}$ denote the transverse fields. Since the slab waveguide has no field variation in the x direction, which we express symbolically by the equation

$$\frac{\partial}{\partial x} = 0 \qquad (4.8)$$

then the operators ∇_t and ∇_t^2 become

$$\nabla_t^2 = \frac{\partial}{\partial y^2} \qquad \text{and} \qquad \nabla_t = \hat{y}\,\frac{\partial}{\partial y}\,.$$

We have shown in Chapter three that the discrete values of the propagation constant ζ for guided modes is limited to the following range

$$k_c < k_s < \zeta_p < k_f$$

which has prompted the definition of the parameters δ, K and γ as

$$\delta = \sqrt{\zeta_p^2 - k_c^2}$$

$$K = \sqrt{k_f^2 - \zeta_p^2}$$

$$\gamma = \sqrt{\zeta_p^2 - k_c^2}$$

Solutions of equation (4.7) provides the expressions for h_z, h_y and e_x in each region (substrate/film/cover). Taking into account the radiation condition as $y \longrightarrow \pm\infty$ the fields in the cover region region are expressed as

$$\left.\begin{aligned} h_z(y) &= A\, e^{-\gamma y} \\ h_y(y) &= \frac{j\zeta}{\gamma}\, A\, e^{-\gamma y} \\ e_x(y) &= \frac{-j\omega\mu}{\gamma}\, A\, e^{-\gamma y} \end{aligned}\right\} \qquad y > 0$$

which consist of waves attenuating in the upward direction. Similarly, in the film region $(-t<y<0)$ the fields are given as

$$\left.\begin{aligned} h_z(y) &= B \sin Ky + C \cos Ky \\ h_y(y) &= \frac{j\zeta}{K}(B \cos Ky - C \sin Ky) \\ e_x(y) &= \frac{-j\omega\mu}{K}(B \cos Ky - C \sin Ky) \end{aligned}\right\} \qquad -t<y<0$$

which consist of standing waves. Finally in the substrate layer ($y<-t$) the fields consist of downward attenuating waves as follows

$$\left.\begin{aligned} h_z(y) &= D\, e^{\delta y} \\ h_y(y) &= \frac{-j\zeta}{\delta} D\, e^{\delta y} \\ e_x(y) &= \frac{j\omega\mu}{\delta} D\, e^{\delta y} \end{aligned}\right\} \qquad y<-t$$

The coefficients A, B, C and D are determined by satisfying the appropriate boundary conditions requiring continuity of tangential electric and magnetic fields at both $y = 0$ and $y = -t$ interfaces. Thus we have

$$h_z(y=0^+) = h_z(y=0^-)$$

$$e_x(y=0^+) = e_x(y=0^-)$$

$$h_z(y=-t^+) = h_z(y=-t^-)$$

$$e_x(y=-t^+) = e_x(y=-t^-)$$

Solving for the transverse electric field in the film region gives

$$e_x(y) = \frac{-j\omega\mu B}{K}\left(\cos Ky - \frac{\gamma}{K}\sin Ky\right) \qquad -t<y<0$$

Hence, the surface-wave field in the film region is expressed as

$$E_x(y,z) = e_x(y)\, e^{\pm j\zeta_p z} = \frac{j\omega\mu B}{K} \left(\frac{\gamma}{K} \sin Ky - \cos Ky\right) e^{\pm j\zeta_p z}$$

If we let $E_0 = \frac{j\omega\mu B}{K}$ be the amplitude of the surface-wave and assume that the impressed field is the forward TE surface-wave mode, the final expression for E_x^i is

$$E_x^i(y,z) = E_0\left(\frac{\gamma}{K} \sin Ky - \cos Ky\right)e^{-j\zeta_p} \qquad (4.9)$$

which establishes the incident TE surface-wave film field.

4.5 MOMENT-METHOD SOLUTION OF THE EFIE:

The previous sections obtained the EFIE for the unknown field in the discontinuity region as well as the surface-wave field incident upon the discontinuity. The EFIE in (4.6) can be solved using the standard method of moments technique. The unknown discontinuity field $E_x(y,z)$ is first expanded in an appropriately chosen set of basis functions $\{e_n\}$

$$E_x(y,z) = \sum_n a_n\, e_n(y,z)$$

where a_n are the unknown expansion coefficients. the EFIE (4.6) for $E_x(y,z)$ is dicretized by substituting the above expansion for unknown E_x. Then rather than forcing (4.6) to be satisfied for all (y,z), it is multiplied by a set of M testing functions $t_m(y,z)$ and the inner products are taken.

$$\sum_n a_n \int_s t_m(y,z)\ e_n(y,z)\ dydz$$

$$- \frac{jk_o}{Z_o} \sum_n a_n \int_s t_m(y,z)\ dydz \int_{s'} \delta n^2(y',z') G_f^e(y|y';z-z')\ e_n(y',z') dy'dz'$$

$$= \int_s t_m(y,z)\ E_x^i(y,z)\ dydz$$

where s,s′ are the longitudinal cross section of the discontinuity parameterized in field/source coordinates. Rearranging the above EFIE leads to

$$\sum_n a_n\ A_{mn} = F_m \qquad \ldots m = 1,2,\ldots,N \tag{4.10}$$

where

$$A_{mn} = \int_s t_m(y,z)\ e_n(y,z)\ dydz$$

$$- \frac{jk_o}{Z_o} \int_s t_m(y,z)\ dydz \int_{s'} \delta n^2(y',z') G_f^e(y|y';z-z')\ e_n(y',z') dy'dz'$$

and the forcing vector F_m is

$$F_m = \int_s t_m(y,z)\ E_x^i(y,z)\ dydz$$

The integral equation (4.6) has now been reduced to an MOM matrix equation (4.10). In the next subsection, a pulse Galerkin's implementation is applied to establish the matrix A_{mn} and the forcing vector F_m.

5.5.1 Pulse Galerkin's Solution:

The discontinuity region is partitioned into N equal sub-area elements ΔS_n centered at (x_n, y_n). The partitioning is defined such that

$$\int_{\ell/2}^{\ell/2} \int_{-t}^{0} dy\, dz = \sum_{n=1}^{N} \Delta S_n$$

Each surface element ΔS_n is defined by (Δy_n) and (Δz_n) which represent the length of the interval spanned by the nth partition along y- and z-direction respectively. Hence we have

$$\Delta y = \frac{t}{N_y} \quad \text{and} \quad \Delta z = \frac{\ell}{N_z}$$

where N_y and N_z are total number of partitions along $\hat{y}$ and $\hat{z}$ respectively.

The basis functions $e_n(y,z)$ and the testing functions $t_m(y,z)$ are chosen to be pulse functions defined as

$$p_n(y,z) = \begin{cases} 1 & \text{....for } (y,z) \in (\Delta S)_n \\ 0 & \text{....otherwise} \end{cases}$$

The index contrast is expanded into a pulse function as well giving

$$\delta n^2(y',z') = \sum_{\ell} \Delta n_\ell^2\, p_\ell(y,z)$$

Hence the term $\delta n^2(y',z')\, e_n(y',z')$ in the expression of the matrix A_{mn} becomes

$$\delta n^2(y',z')\, e_n(y',z') = \Delta n_n^2\, p_n(y',z')$$

With all this in mind, substituting the expressions for the basis functions and the testing functions in A_{mn} and F_m gives

$$A_{mn} = \delta_{mn}\Delta S - \frac{jk_0}{Z_0}\Delta n_n^2 \int_{(\Delta S)_m} dy\, dz \int_{(\Delta S)_n} G_f^e(y|y';z-z')\, dy'dz'$$

$$F_m = \int_{(\Delta S)_m} E_x^i(y,z)\, dy\, dz$$

We now proceed in evaluating the above spatial integrals required in spectral integral representation of MOM matrix elements. Note that $(\Delta S)_n$ is defined by $(y_n - \frac{\Delta y}{2}) < y < (y_n + \frac{\Delta y}{2})$ and $(z_n - \frac{\Delta z}{2}) < z < (z_n + \frac{\Delta z}{2})$. We can see from the expression of $G_f^e(y|y';z-z')$ in (4.2) that the integral over the z-coordinate is

$$\phi_z^{mn}(\zeta) = \int_{z_m-\frac{\Delta z}{2}}^{z_m+\frac{\Delta z}{2}} dz \int_{z_n-\frac{\Delta z}{2}}^{z_n+\frac{\Delta z}{2}} e^{j\zeta|z-z'|}\, dz'$$

$$= \begin{cases} \dfrac{2(1-\cos\zeta\Delta z)}{\zeta^2}\, e^{j\zeta|z_m-z_n|} & \text{.....for } m\neq n \\[2ex] \dfrac{j2\Delta z}{\zeta} + \dfrac{2}{\zeta^2}\,(1- e^{j\zeta\Delta z}) & \text{.....for } m=n \end{cases}$$

The integrals over the y-coordinate are summarized as follows

$$\phi_{yo}^{mn}\left\{\begin{matrix}\sigma\\ K\end{matrix}\right\} = \int_{y_m-\frac{\Delta y}{2}}^{y_n+\frac{\Delta y}{2}} dy \int_{y_n-\frac{\Delta y}{2}}^{y_n+\frac{\Delta y}{2}} dy' \ \cos\left\{\begin{matrix}\sigma\\ K\end{matrix}\right\}(y_m-y_n)$$

$$= \frac{2(1-\cos\left\{\begin{matrix}\sigma\\ K\end{matrix}\right\})\Delta y}{\left\{\begin{matrix}\sigma^2\\ K^2\end{matrix}\right\}} \cos\left\{\begin{matrix}\sigma\\ K\end{matrix}\right\}(y_m-y_n)$$

$$\phi_{y1}^{mn}\left\{\begin{matrix}\sigma\\ K\end{matrix}\right\} = \int_{y_m-\frac{\Delta y}{2}}^{y_n+\frac{\Delta y}{2}} dy \int_{y_n-\frac{\Delta y}{2}}^{y_n+\frac{\Delta y}{2}} dy' \ e^{j\left\{\begin{matrix}\sigma\\ K\end{matrix}\right\}(y+y')}$$

$$= \frac{2(1-\cos\left\{\begin{matrix}\sigma\\ K\end{matrix}\right\})\Delta y}{\left\{\begin{matrix}\sigma^2\\ K^2\end{matrix}\right\}} e^{j\left\{\begin{matrix}\sigma\\ K\end{matrix}\right\}(y_m+y_n)}$$

The final form for the spectral integral representation for the MOM matrix A_{mn} can now be written in terms of the above functions as follows

$$A_{mn} = \delta_{mn}\Delta S - jk_0^2\Delta n_n^2 \left\{ j\phi_z^{mn}(-\zeta_p) \left[B_1(\zeta_p)\ \phi_{y1}^{mn}(-K)\ e^{-jKt} + \right.\right.$$

$$\left. 2B_2(\zeta_p)\ \phi_{yo}^{mn}(K)\ e^{-jKt} + B_3(\zeta_p)\ \phi_{y1}^{mn}(K)\ e^{jKt} \right]$$

$$+ \frac{1}{2\pi}\int_0^{k_0\sqrt{n_s^2-n_c^2}} \left[\phi_{yo}^{mn}(\sigma(\gamma)) \right.$$

$$+ \mathrm{Re}\left\{ R_+^{(1)}\ \phi_{y1}^{mn}(-\sigma(\gamma))e^{-j2\sigma t}\right\}$$

$$+ 2\mathrm{Re}\left\{ R_+^{(2)}\ \phi_{yo}^{mn}(\sigma(\gamma))e^{-j2\sigma t}\right\}$$

$$\left. + \mathrm{Re}\left\{ R_-^{(2)}\ \phi_{y1}^{mn}(\sigma(\gamma))\right\} \right] \phi_z^{mn}(\sigma(\gamma))\ \frac{\gamma\ d\gamma}{\sigma(\gamma)\zeta(\gamma)}$$

$$+ \int_0^{\infty} \left[\phi_{yo}^{mn}(\sigma(\rho)) + \mathrm{Re}\left\{ R_+^{(1)}\ \phi_{y1}^{mn}(-\sigma(\rho))e^{-j2\sigma t}\right\}\right.$$

$$+ 2\mathrm{Re}\left\{ R_+^{(2)}\ \phi_{yo}^{mn}(\sigma(\rho))e^{-j2\sigma t}\right\}$$

$$\left.\left. + \mathrm{Re}\left\{ R_-^{(2)}\phi_{y1}^{mn}(\sigma(\rho))\right\} \right]\phi_z^{mn}(\sigma(\rho))\ \frac{\rho\ d\rho}{\sigma(\rho)\zeta(\rho)} \right\} \tag{4.11}$$

where the coefficients B_1, B_2, B_3, $R_+^{(1)}$, $R_+^{(2)}$ and $R_-^{(2)}$ are defined in chapter three. The forcing vector F_m is computed in the same way and found to be

$$F_m = \frac{4e^{-j\zeta_p z_m}}{\zeta_p K} \sin(K\frac{\Delta y}{2})\ \sin(\zeta_p \frac{\Delta z}{2}) \left[\frac{\gamma}{K} \sin(Ky_m) - \cos(Ky_m) \right] \tag{4.12}$$

Once the matrix elements of A_{mn} are known as well as the forcing vector F_m, the matrix equation (4.10) is inverted numerically to quantify the a_n's; the unknown induced field $E_x(y,z)$ is subsequently known. Matrix elements in (4.11) can be calculated analytically in closed form except for the spatial frequency integration over the continuous spectrum which must be implemented numerically.

4.5.2 Scattering Coefficients

In this section, the scattering coefficients i.e reflection and transmission coefficients, are evaluated using the pulse function expansion for the induced field in the discontinuity region found previously. In fact, the scattered field (reflected or transmitted) is given by (4.5). The surface wave scattered field is expanded in terms of the discrete part of the electric Green's function as follows

$$E_x^{SW}(y,z) = j\omega\varepsilon_0 \int_{S'} \delta n^2(y',z')\, G_{pole}(y|y';z-z')\, E_x(y',z')\, dy'dz'$$

The back scattered field or reflected wave E_x^{BS} is defined as the surface scattered wave for source points greater than the field points along the z-direction, i.e $z <$ all z'; whereas for the forward scattered wave we have $z >$ all z'. The transmitted wave E_x^T is defined as the incident wave augmented by the forward scattered wave. The reflection coefficient is expressed as the back scattered wave divided by the incident wave, all evaluated at the input plane along the z-direction of the discontinuity, i.e at $z = -\ell/2$. Thus we have

$$R = \left. \frac{E_x^{BS}(y,z)}{E_x^{i}(y,z)} \right|_{z = -\ell/2} \qquad (4.13)$$

The transmission coefficient is expressed as the transmitted wave evaluated at the output plane ($z=\ell/2$), divided by the incident wave evaluated at the input plane of the discontinuity

$$T = \frac{E_x^T(y,z)\,|\,z = \ell/2}{E_x^i(y,z)\,|\,z = -\ell/2}$$

Since the surface-wave scattered field E_x^{sw} depends on the discrete electric Green's function, we expect that G^e_{pole} has the same functional dependence on y as the incident field. This latter derivation is lengthy and the result is given as

$$G^e_{pole}(y|y';z-z') = \frac{jk_oZ_oN_o}{A_o}\left[\frac{\gamma}{K}\,\sin Ky'-\cos Ky\right]\left[\frac{\gamma}{K}\,\sin Ky-\cos Ky\right]\,e^{-j\zeta_p|z-z'|} \tag{4.14}$$

where A_o and N_o are defined as

$$A_o = 4\zeta_p k_o^2\sqrt{(n_f^2-n_s^2)(n_f^2-n_c^2)}\;(\gamma+\delta+\gamma\delta t)$$

$$N_o = \frac{4j\,[K^4\gamma\delta+K^2\gamma\delta^3]}{\sqrt{K^4+\gamma^2\delta^2+K^2(\gamma^2+\delta^2)}}$$

Substituting the pulse function expansion for the discontinuity field $E_x(y,z)$ and using (4.14) for the discrete Green's function, in the expression for the forward and backscattered field leads to the final expression for the reflection and transmission coefficients as follows

$$R = \frac{-4k_o^2 N_o}{A_o E_o \zeta_p K} e^{-j\zeta_p \ell} \sin(K\frac{\Delta y}{2}) \sin(\zeta_p \frac{\Delta z}{2})\ \Delta n^2 \sum_n a_n (\frac{\gamma}{K} \sin K y_n - \cos K y_n) e^{-j\zeta_p z_n}$$

$$T = e^{-j\zeta_p \ell} \left[1 - \frac{4k_o^2 N_o}{A_o E_o \zeta_p K} e^{-j\zeta_p \ell} \sin(K\frac{\Delta y}{2}) \sin(\zeta_p \frac{\Delta z}{2})\ \Delta n^2 \sum_n a_n (\frac{\gamma}{K} \sin K y_n - \cos K y_n) e^{j\zeta_p z_n} \right]$$

4.5.3 Numerical Results

A study of scattering parameters (reflection, transmission and power radiated) permits to know the behavior of the waveguide in the presence of the discontinuity region. The waveguiding structure is chosen such that there is a 5% refractive index contrast between film and substrate, and a 10% contrast between film and cover regions. The normalized width t/λ of the guiding region is chosen such that only the TE_1 surface-wave mode is excited; all other modes are at cutoff. This specific value of t/λ is extracted from the dispersion curve of the waveguide.

Curves of scattering parameters versus the discontinuity refractive index are illustrated by Figure 14 and 15. To ensure mono-mode surface-wave propagation, t/λ must be equal to 0.5 and 1.2 for the case of GaAs film region (n_f = 3.2) and glass (n_f =1.5), respectively. It is apparent that for small contrast between the film and the discontinuity region, we obtain small reflection (less than 20%). As the contrast Δn^2 gets higher, the reflection coefficient gets bigger (up to 60%).

Figures 16 through 19 show the scattering parameters versus the normalized length of the discontinuity along the z-axis. It appears that when the discontinuity gets longer the transmission coefficient gets lower. This is in agreement with our physical intuition.

In Figures 20 through 21, relative field amplitude $|E_x(y,z)/E_{max}|$ versus normalized length y/t are shown. We can see that the field distribution is asymmetric with respect to y = -0.5t axis. This is expected since we are dealing with an asymmetric slab waveguide.

4.6 SUMMARY

A polarization EFIE description of the discontinuity region along an asymmetric slab waveguide is developed. An equivalent polarization description of the dielectric discontinuity is obtained in terms of the contrast of its refractive index against that of the unperturbed surface waveguide. Hence we have

$$\vec{J}_{eq}(\vec{r}) = j\omega\varepsilon_0 \delta n^2(\vec{r})\ \vec{E}(\vec{r})$$

The fields excited within the discontinuity consist of the impressed field of an incident wave augmented by the scattered field maintained by the equivalent current

$$E_x(y,z) = E_x^s(y,z) + E_x^i(y,z)$$

Rearranging leads to the EFIE

$$E_x(y,z) - j\frac{k_0}{Z_0}\int_{LCS} \delta n^2(y',z')G_f^e(y|y';z-z')E_x(y',z')dy'dz' = E_x^i(y,z)$$

where $E_x^i(y,z)$ consists of a single forward propagating TE_1 surface-wave mode and expressed as

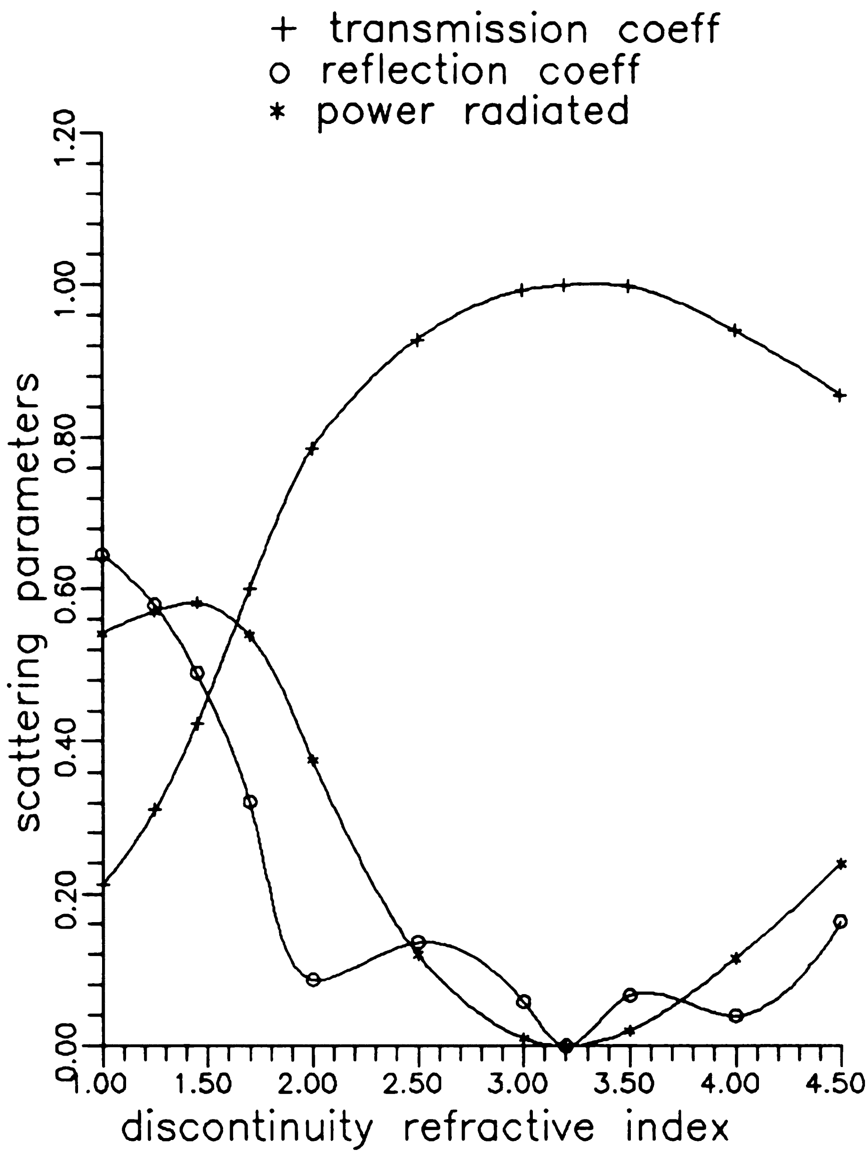

Figure 14: Scattering parameters Vs uniform refractive index of the slice discontinuity with $t/\lambda=.5$ $l/t=.5$ $n_f=3.2$(GaAs) $n_s=3.04$ $n_c=2.88$

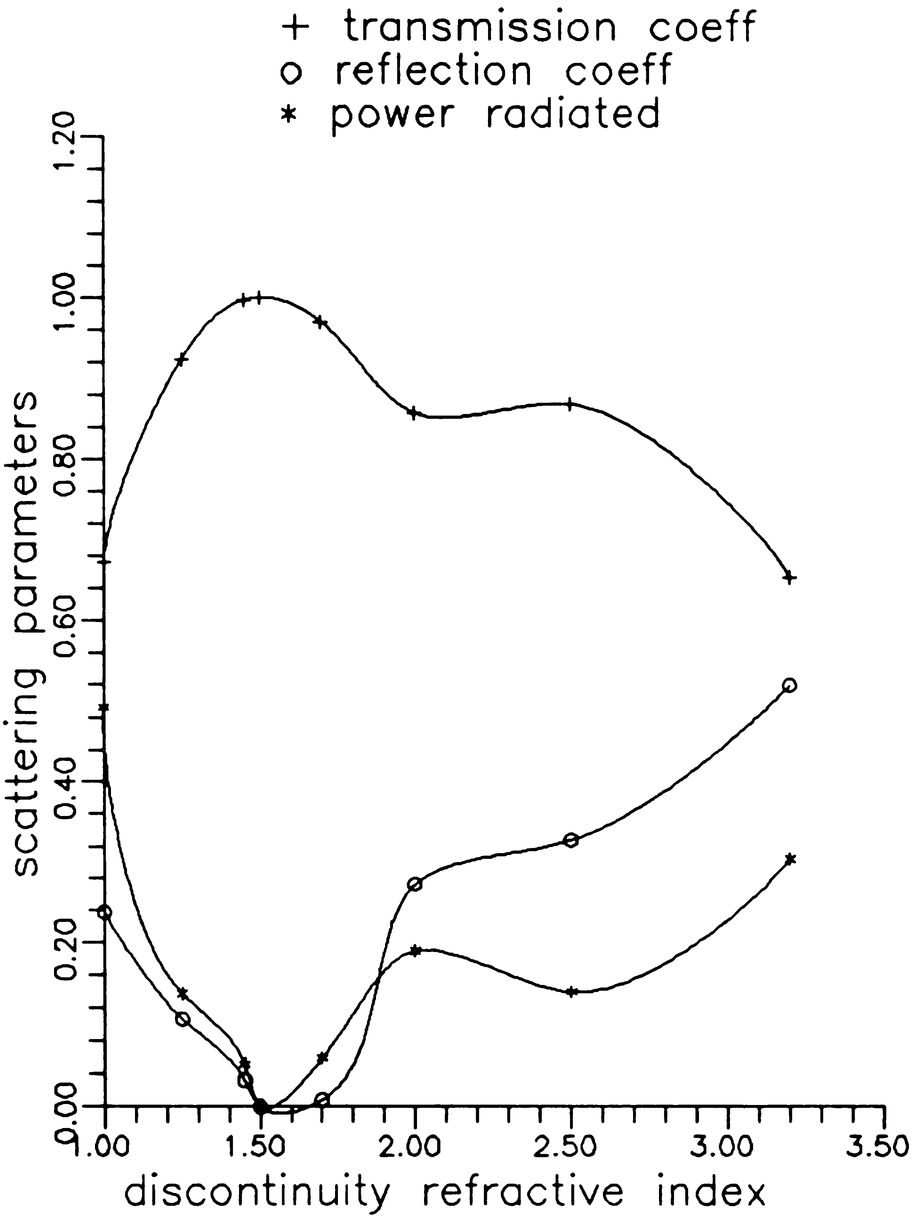

Figure 15: Scattering parameters Vs uniform refractive index of the slice discontinuity with $t/\lambda=1.2$ $l/t=0.75$ $n_f=1.5$(glass) $n_s1.425$ $n_c=1.35$

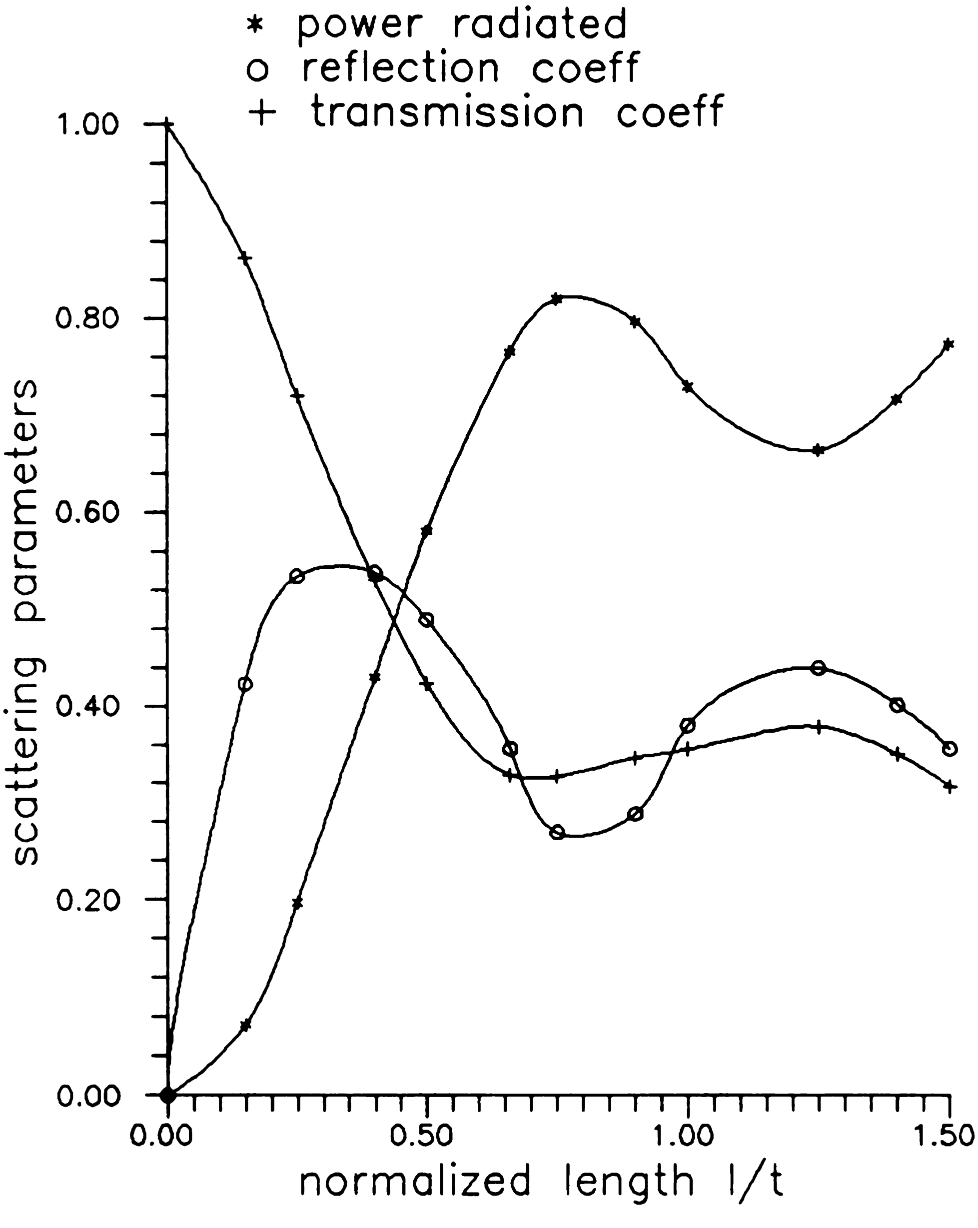

Figure 16: Scattering parameters Vs normalized length along z–axis with $t/\lambda=0.5$ $n_f=3.2$ (GaAs) $n_s=3.04$ $n_c=2.88$ $n_d=1.45$

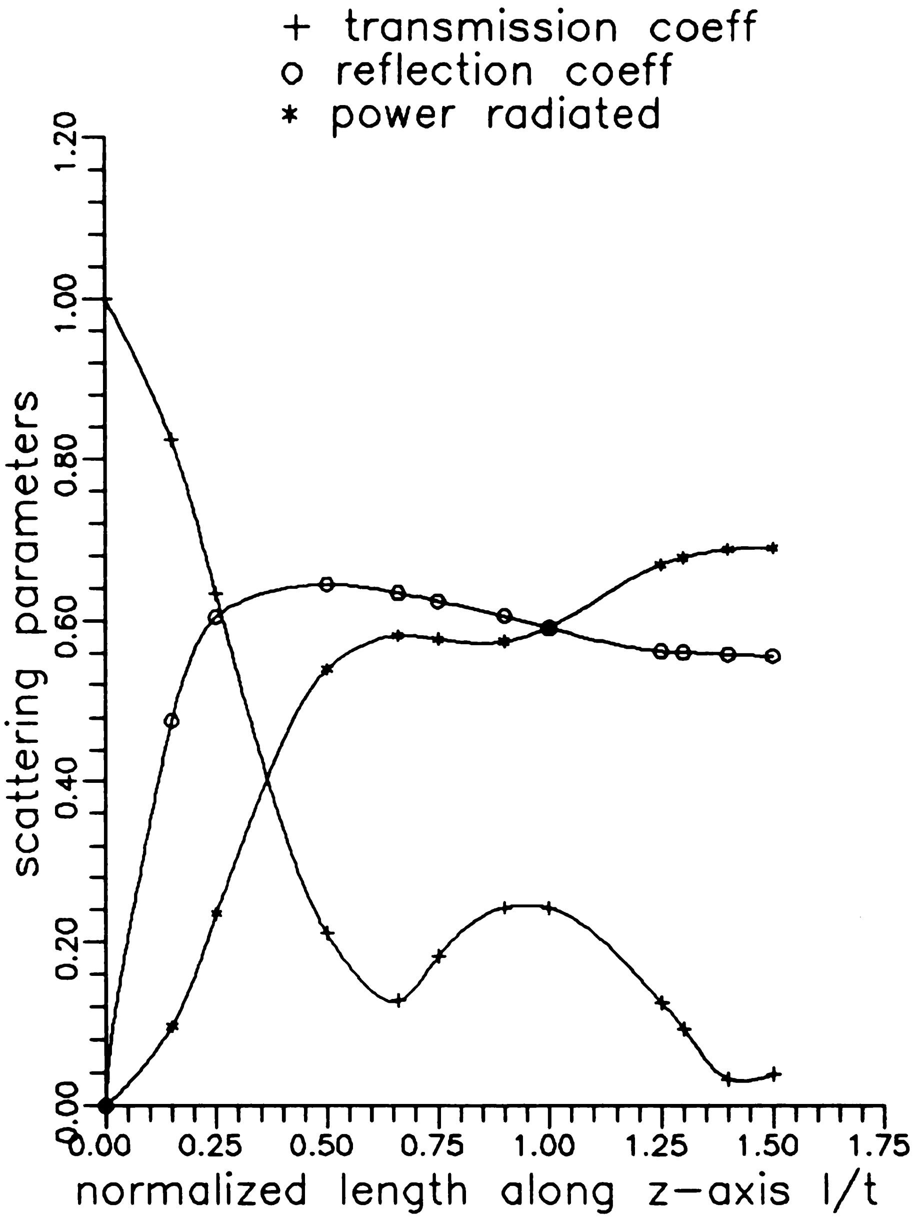

Figure 17: Scattering parameters Vs normalized length of the slice discontinuity with $t/\lambda=.5$ $n_f=3.2$(GaAs) $n_s=3.04$ $n_c=2.88$ $n_d=1.$(air)

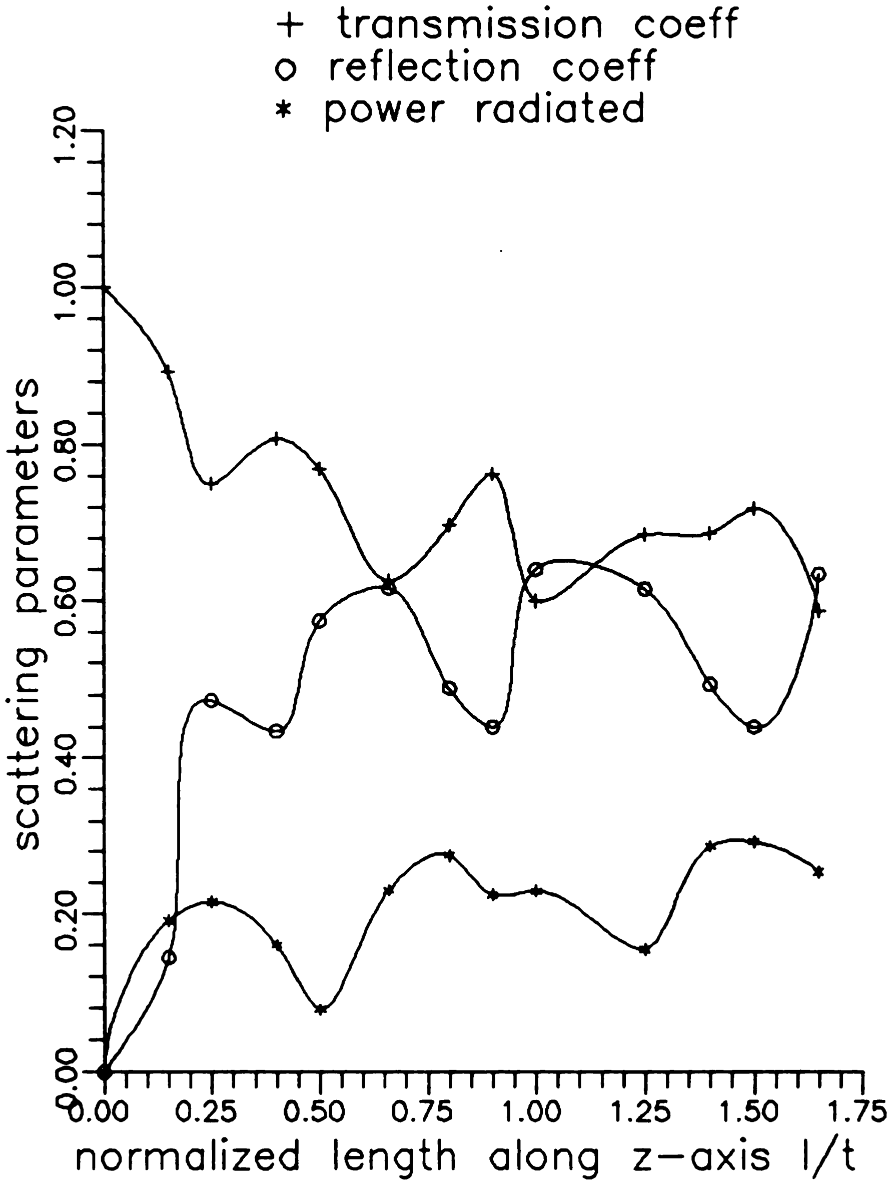

Figure 18: Scattering parameters Vs normalized length of the slice discontinuity with $t/\lambda=1.2$ $n_f=1.5$ $n_s=1.425$ $n_c=1.35$ $n_d=3$.

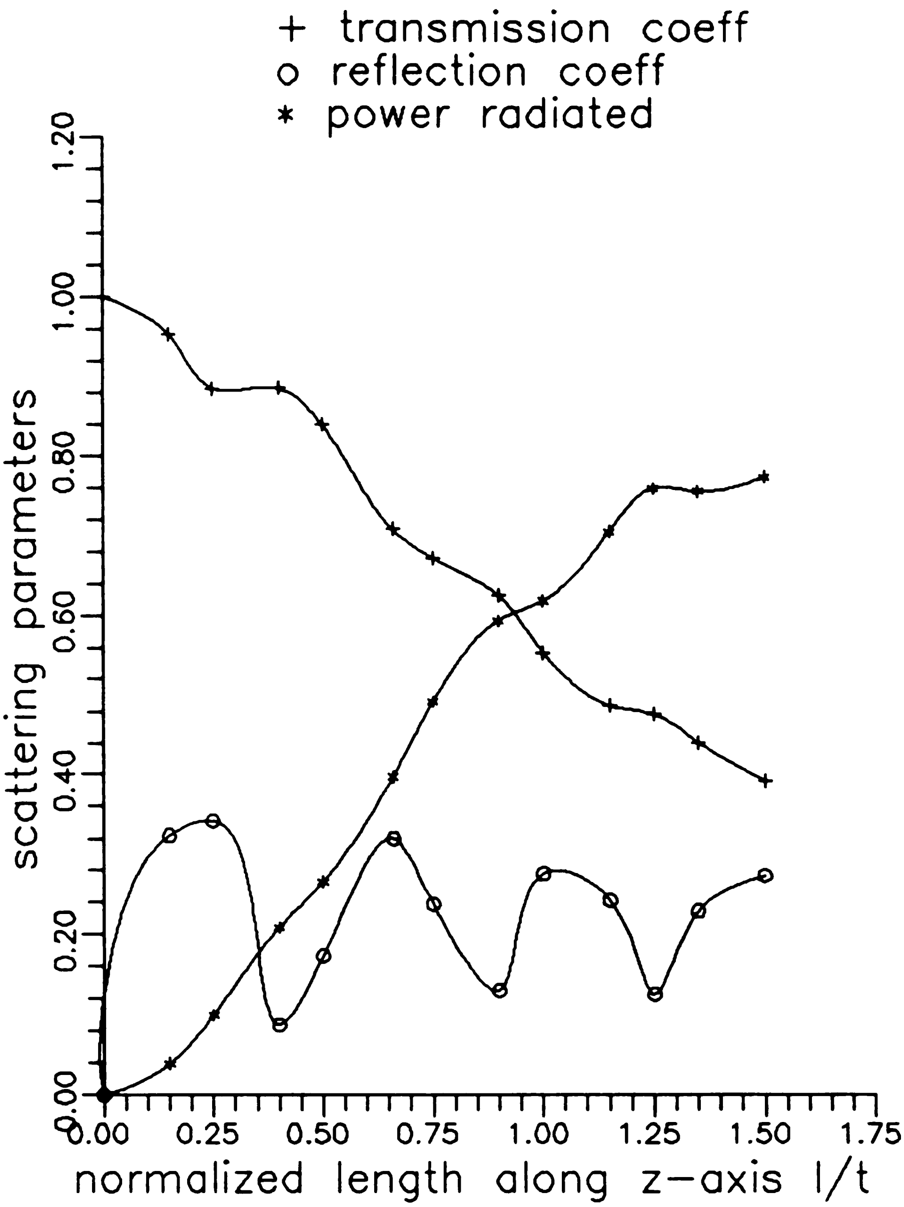

Figure 19: Scattering parameters Vs normalized length of the slice discontinuity with $t/\lambda=1.2$ $n_f=1.5$ $n_s=1.425$ $n_c=1.35$ $n_d=1$.

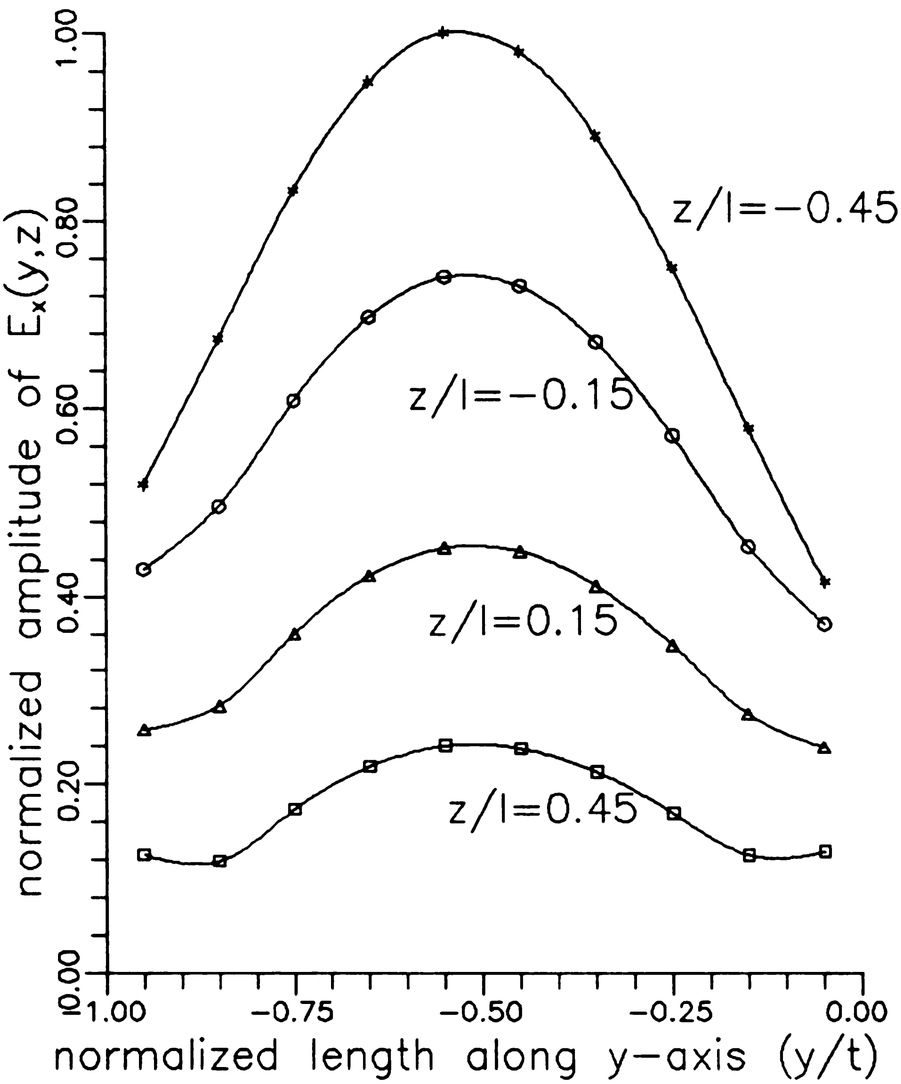

Figure 20 : Distribution of field $E_x(y,z)$ excited in dielectric discontinuity region with TE_1 incident mode wave $n_f=1.5$ $n_s=1.425$ $n_c=1.35$ $t/\lambda=1.2$ $l/t=.5$ $n_d=1.$

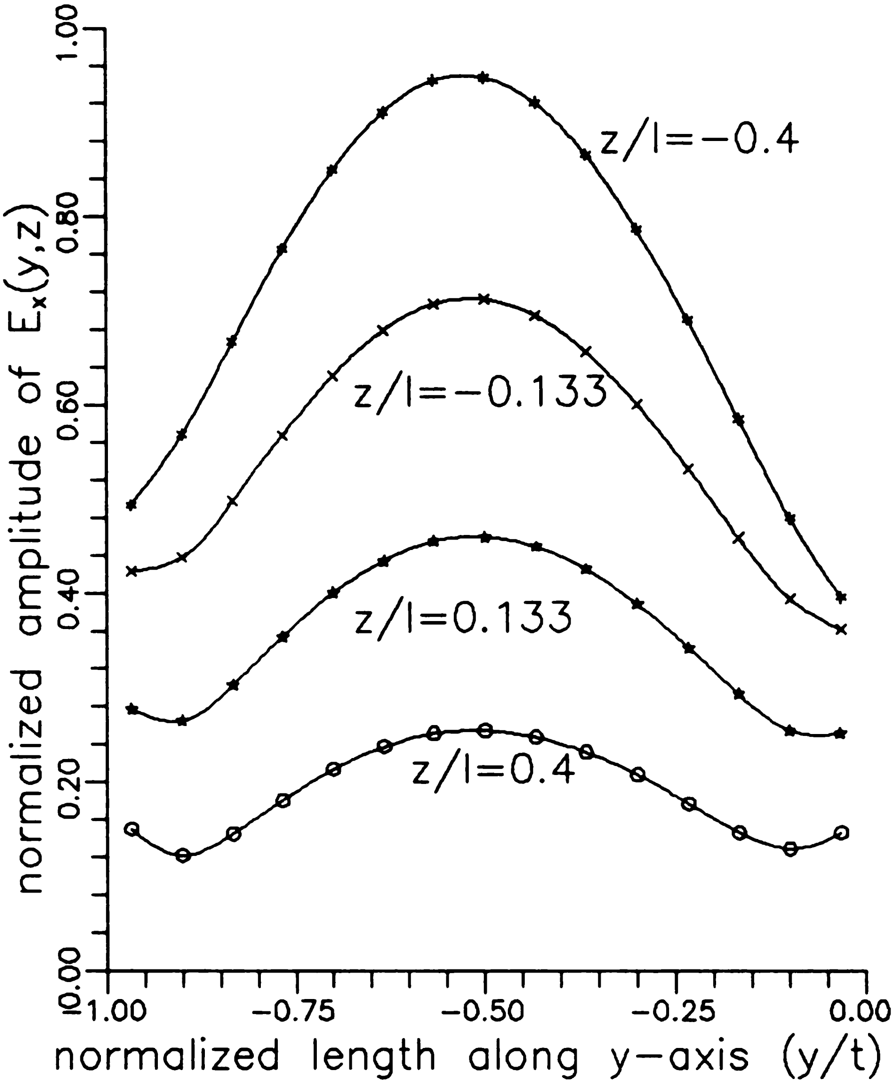

Figure 21 : Distribution of field $E_x(y,z)$ excited in dielectric discontinuity region with TE_1 incident mode wave $n_f=3.2$ $n_s=3.04$ $n_c=2.88$ $t/\lambda=0.5$ $l/t=.5$ $n_d=1.$

$$E_x^i(y,z) = E_0(\frac{\gamma}{K} \sin Ky - \cos Ky)e^{-j\zeta_p}$$

The EFIE is solved using the standard method of moments technique. The unknown discontinuity field is expanded into a pulse function expansion. The EFIE is reduced to an MOM matrix equation. A pulse Galerkin's implementation is used to establish the MOM matrix.

Chapter Five

CONCLUSIONS

A detailed development of the electric Hertz potential Green's function for a tri-layered substrate/film/cover dielectric structure was presented in chapter two. The electric Green's function is a constant multiple of the Hertz potential Green's function due to the x-invariance of the fields. This development demanded a mathematically rigorous treatment and revealed that the electric Green's function is represented by 1-D spectral integral, which is alternatively evaluated by contour deformation.

In chapter three, complex-plane analysis applied to the spectral integral representation of the electric Green's function leaded to the identification of the propagation mode spectrum of the asymmetric planar dielectric waveguide. A discrete mode spectrum was shown to arise from integrating around the surface-wave poles, while hyperbolic branch cuts corresponded to a continuous spectrum. This electric Green's function was specialized for the case of symmetric slab. It was found that it agrees completely with Rozzi's result [1,14]. In fact, after shifting the axis and some tedious manipulations, our specialized Green's function reduces to the TE even Rozzi's Green's function for the symmetric slab waveguide. This is detailed in appendix E.

Finally, a polarization EFIE description of a discontinuity region along an asymmetric slab was developed. Standard method of moments(MOM) numerical solution were obtained for discontinuity field, leading to scattering coefficients and the fractional radiated power.

APPENDICES

APPENDIX A

APPENDIX A

Electric Hertzian potential

Using $\nabla\cdot\vec{H} = 0$ (non existence of magnetic monopoles) the magnetic field $\vec{H}$ can be expressed as the curl of a vector potential. In an electrically homogeneous medium, $\vec{H}$ may be expressed in terms of the Hertzian potential $\vec{\Pi}$ as

$$\vec{H} = j\omega\varepsilon\ \nabla\times\vec{\Pi} \tag{1}$$

From Faraday's law we have

$$\nabla\times\vec{E} = -j\omega\mu\ \vec{H}$$

Substituting (1) into Faraday's law yields

$$\nabla\times(\vec{E} - k^2\vec{\Pi}) = 0 \tag{2}$$

where $k^2 = \omega^2\mu\varepsilon$ is the wavenumber in the medium. Equation (2) implies

$$\vec{E} = k^2\vec{\Pi} - \nabla\varphi \tag{3}$$

where φ is a suitable scalar field. Using (1) and (3) into Ampere's law

$$\nabla\times\vec{H} = \vec{J} + j\omega\varepsilon\vec{E}$$

yields

$$(\nabla^2 + k^2)\vec{\Pi} = \frac{-\vec{J}}{j\omega\varepsilon} + \nabla(\nabla\cdot\vec{\Pi} + \varphi) \tag{4}$$

where we used the vector identity $\nabla\times\nabla\times\vec{A} = \nabla\nabla\cdot\vec{A} - \nabla^2\vec{A}$. Since a vector field is uniquely determined through knowledge of its curl and divergence, by choosing $\nabla\cdot\vec{\Pi} = -\varphi$ uniquely determines $\vec{\Pi}$. Thus (4) simplifies to

$$(\nabla^2 + k^2)\vec{\Pi} = \frac{-\vec{J}}{j\omega\varepsilon}$$

which consists of the Helmholtz equation for the Hertzian potential subject to the Lorentz gauge $\nabla\cdot\vec{\Pi} = -\varphi$. Use of this Gauge in (3) yields

$$\vec{E} = (k^2 + \nabla\nabla\cdot)\vec{\Pi}$$

which relates the electric field to the Hertz potential.

APPENDIX B

APPENDIX B

Primary Green's Function

The principal Hertzian potential satisfies the following Helmholtz equation

$$\frac{\partial^2 \pi^p_{xi}}{\partial y^2} - p_i^2 \pi^p_{xi}(y,\zeta) = \frac{-j_x}{j\omega\varepsilon_i}$$

π^p_{xi} can be written in terms of a primary Green's function in transform domain

$$\pi^p_{xi}(y,\zeta) = \int_{\infty}^{+\infty} \frac{j_x(y,\zeta)}{j\omega\varepsilon_i}\, g_i^p(y|y';\zeta)\, dy'$$

where $g_i^p(y|y';\zeta)$ satisfies

$$\frac{\partial^2 g_i^p}{\partial y^2} - p_i^2 g_i^p = -\delta(y-y') \qquad (1)$$

We perform a Fourier transformation on the y-axis. we define the Fourier transform pair $f(y) \longleftrightarrow \tilde{f}(\eta)$. Hence $\tilde{g}_i^p(\eta,\zeta)$ and $g_i^p(y,\zeta)$ are defined as

$$\tilde{g}_i^p(\eta,\zeta) = \int_{\infty}^{+\infty} g_i^p(y,\zeta)\; e^{-j\eta y}\; dy$$

and

$$g_i^p(y,\zeta) = \frac{1}{2\pi}\int_{\infty}^{+\infty} \tilde{g}_i^p(\eta,\zeta)\; e^{j\eta y}\; d\eta \qquad (2)$$

Substitute (2) into (1) yields

$$\left[\frac{\partial^2}{\partial y^2} - p_i^2 \right] \frac{1}{2\pi} \int_{-\infty}^{+\infty} \tilde{g}_i^p(\eta,\zeta)\, e^{j\eta y}\, d\eta = -\delta(y-y')$$

$$= \frac{-1}{2\pi} \int_{-\infty}^{+\infty} e^{j\eta(y-y')}\, d\eta$$

Rearranging the above equation yields

$$\int_{-\infty}^{+\infty} \left\{ [\eta^2 + p_i^2]\, \tilde{g}_i^p(\eta,\zeta) - e^{-j\eta y'} \right\} e^{j\eta y}\, d\eta = 0 \qquad (3)$$

We can see that (3) is the inverse Fourier transformation of the quantity in brackets.

Since $\mathcal{F}_y^{-1}\{\cdots\} = 0 \Rightarrow \{\cdots\} = 0$

$$\text{Hence } \tilde{g}_i^p(\eta,\zeta) = \frac{e^{-j\eta y'}}{\eta^2 + p_i^2} \qquad (4)$$

Use of (2) and (4) yields to the primary Green's function in axial transform domain

$$g_i^p(y,\zeta) = \frac{1}{2\pi} \int_{-\infty}^{+\infty} \frac{e^{j\eta(y-y')}}{\eta^2 + p_i^2}\, d\eta$$

$$= \frac{1}{2\pi} \int_{-\infty}^{+\infty} \frac{e^{j\eta(y-y')}}{(\eta - jp_i)(\eta + jp_i)}\, d\eta \qquad (5)$$

We apply a deformation of this real line integration and apply Cauchy's theorem

$$\int_C (\cdots)\, d\eta = 0$$

where $C = C_o + C_p^{\pm} + C_\infty^{\pm}$ is the deformation contour. C_o is the initial real line contour along the $\mathrm{Re}\{\eta\}$ axis. $C_p^{\pm}$ is the pole contour. Note that the integrand in (5) has two simple poles at $\eta = \pm jp_i$ $i = f,c$ for sources immersed in the film and cover region respectively. We specialize our solution for $y' = 0$ since the final result can be shifted to any $y' \neq 0$. Hence we can write

$$g_i^p(y,\zeta) = \frac{1}{2\pi} \int_{\infty}^{+\infty} \frac{e^{j\eta y}}{(\eta - jp_i)(\eta + jp_i)} \, d\eta \tag{6}$$

The exponential factor $e^{j\eta y}$ appears as part of the integrand in (6). Writing $\eta = \eta_r + j\eta_i$ the above exponential factor will be

$$e^{j\eta y} = e^{-\eta_i y} \, e^{j\eta_r y}$$

Therefore to ensure convergence of the integrand, we perform an upper half closure for $y > 0$ and a lower half closure for $y < 0$. This is shown in Figure 22.

$$\int_{C_\infty^{\pm}} (\cdots) \, d\eta = 0 \qquad \text{since the integrand converges}$$

Hence, for $y > 0$:

$$\int_{\infty}^{+\infty} \frac{e^{j\eta y}}{\eta^2 + p_i^2} \, d\eta = 2\pi j \left. \frac{e^{j\eta y}}{(\eta + jp_i)} \right|_{\eta = jp_i}$$

then

$$g_i^p(y,\zeta) = \frac{e^{-p_i y}}{2p_i} \qquad \ldots y > 0$$

and for $y > 0$

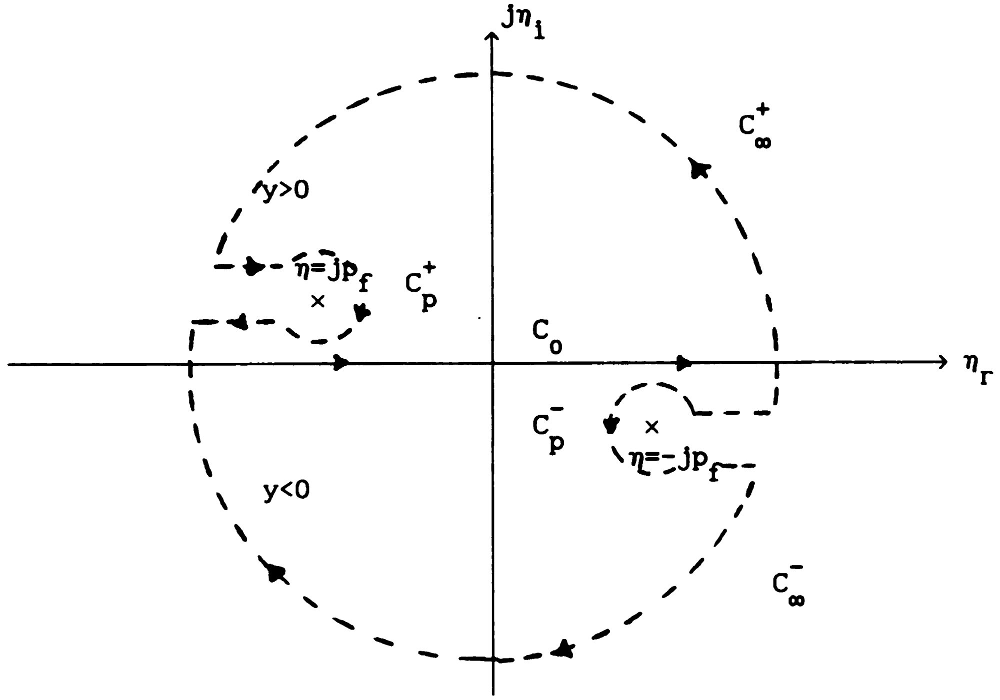

Figure 22: Complex η-plane.

$$\int_{-\infty}^{+\infty} \frac{e^{j\eta y}}{\eta^2+p_i^2}\, d\eta = -2\pi j \left. \frac{e^{j\eta y}}{(\eta - jp_i)} \right|_{\eta = -jp_i}$$

then

$$g_i^p(y,\zeta) = \frac{e^{p_i y}}{2p_i} \qquad \ldots y < 0$$

Therefore

$$g_i^p(y,\zeta) = \frac{e^{-p_i|y|}}{2p_i} \qquad \text{for all } y$$

Shifting the result to $y' \neq 0$ yields to the final form for the primary Green's function in axial transform domain

$$g_i^p(y,\zeta) = \frac{e^{-p_i|y-y'|}}{2p_i}$$

APPENDIX C

APPENDIX C

Application of Boundary Conditions

Enforcing tangential $\vec{e}$ at the interfaces requires

$$\pi_{xc}(o,\zeta) = N_{fc}^2\pi_{xf}(o,\zeta) \tag{1}$$

and

$$\pi_{xf}(-t,\zeta) = N_{sf}^2\pi_{xs}(-t,\zeta) \tag{2}$$

In a similar fashion, continuity of tangential $\vec{h}$ yields

$$\frac{\partial\pi_{xc}(o,\zeta)}{\partial y} = N_{fc}^2\frac{\partial\pi_{xf}(o,\zeta)}{\partial y} \tag{3}$$

$$\frac{\partial\pi_{xf}(-t,\zeta)}{\partial y} = N_{sf}^2\frac{\partial\pi_{xs}(-t,\zeta)}{\partial y} \tag{4}$$

The total potential in the film region consists of the sum of a primary component augmented by a reflected part and is expressed as

$$\pi_{xf}(y,\zeta) = w_{xf}^{r+}\, e^{-p_f y} + w_{xf}^{r-}\, e^{p_f y} + \int_{-\infty}^{+\infty}\frac{j_x(y',\zeta)}{j\omega\varepsilon_f}\,\frac{e^{-p_f|y-y'|}}{2p_f}\,dy'$$

Apllication of boundary condition (1) at y = 0 interface gives

$$w_{xc}^{t} - N_{fc}^2(w_{xf}^{r+} + w_{xf}^{r-}) = N_{fc}^2\int_{-\infty}^{+\infty}\frac{j_x(y',\zeta)}{j\omega\varepsilon_f}\,\frac{e^{p_f y'}}{2p_f}\,dy'$$

We used the fact that $|y-y'| = y-y'$ since all $y > y'$ near $y = 0$, that is all field points are greater than source points. We define $V_y(\zeta)$ as follows

$$V_y(\zeta) = \int_{\infty}^{+\infty} \frac{J_x(y',\zeta)}{j\omega\varepsilon_f} \frac{e^{p_f y'}}{2p_f} dy'$$

Hence boundary condition (1) yields

$$N_{cf}^2 w_{xc}^t - w_{xf}^{r+} - w_{xf}^{r-} = V_y(\zeta) \tag{5}$$

In the same fashion boundary condition (2) yields

$$N_{cf}^2 w_{xC}^t + \frac{p_f}{p_c} (w_{xf}^{r-} - w_{xf}^{r+}) = \frac{p_f}{p_c} V_y(\zeta) \tag{6}$$

Near y = -t interface all y < y', hence boundary condition (3) at y = -t interface yields

$$-w_{xf}^{r+} e^{p_f t} - w_{xf}^{r-} e^{-p_f t} + N_{sf}^2 w_{xs}^t e^{-p_s t} = e^{-p_f t} W_y(\zeta) \tag{7}$$

where $W_y(\zeta)$ is defined as

$$W_y(\zeta) = \int_{\infty}^{+\infty} \frac{J_x(y',\zeta)}{j\omega\varepsilon_f} \frac{e^{-p_f y'}}{2p_f} dy'$$

Similarly, boundary condition (4) gives

$$\frac{p_f}{p_s} (w_{xf}^{r+} e^{p_f t} - w_{xf}^{r-} e^{-p_f t}) + N_{sf}^2 w_{xs}^t e^{-p_s t} = \frac{p_f}{p_s} e^{-p_f t} W_y(\zeta) \tag{8}$$

First, we eliminate w_{xc}^t between (5) and (6) leading to

$$w_{xf}^{r+} (1- \frac{p_f}{p_c}) + w_{xf}^{r-} (1+ \frac{p_f}{p_c}) = V_y(\zeta) (\frac{p_f}{p_c} - 1) \tag{9}$$

Secondly, we eliminate w_{xs}^t between (7) and (8) leading to

$$w_{xf}^{r+} (\frac{p_f}{p_s} + 1) e^{p_f t} + w_{xf}^{r-} (1 - \frac{p_f}{p_s}) e^{-p_f t} = W_y(\zeta) (\frac{p_f}{p_s} - 1) e^{-p_f t} \tag{10}$$

Combining (9) and (10) and after some manipulations, the expressions for w_{xf}^{r+} and w_{xf}^{r-} are as follows

$$w_{xf}^{r+} = R_{+}^{(1)} e^{-2p_f t}\, W_y(\zeta) + R_{+}^{(2)} e^{-2p_f t}\, V_y(\zeta) \tag{11}$$

$$w_{xf}^{r-} = R_{-}^{(1)} e^{-2p_f t}\, W_y(\zeta) + R_{-}^{(2)} V_y(\zeta) \tag{12}$$

where $R_{+}^{(1)}$, $R_{+}^{(2)}$, $R_{-}^{(1)}$ and $R_{-}^{(2)}$ are defined below

$$R_{+}^{(1)} = \frac{(p_f+p_c)(p_f-p_s)\, e^{p_f t}}{2\cosh(p_f t)\ [(p_f^2+p_c p_s)\tanh(p_f t)+p_f(p_s+p_c)]}$$

$$R_{+}^{(2)} = \frac{(p_f-p_s)(p_f-p_c)\, e^{p_f t}}{2\cosh(p_f t)\ [(p_f^2+p_c p_s)\tanh(p_f t)+p_f(p_s+p_c)]}$$

$$R_{-}^{(1)} = R_{+}^{(2)}$$

$$R_{-}^{(2)} = \frac{(p_f+p_s)(p_f-p_c)\, e^{p_f t}}{2\cosh(p_f t)\ [(p_f^2+p_c p_s)\tanh(p_f t)+p_f(p_s+p_c)]}$$

Substitute the expressions of $V_y(\zeta)$ and $W_y(\zeta)$ in (11) and (12) gives the final expressions for w_{xf}^{r+} and w_{xf}^{r-} as follows

$$w_{xf}^{r+} = \int_{-\infty}^{+\infty} \frac{j_x(y',\zeta)}{2j\omega\varepsilon_f p_f} \left(R_{+}^{(1)} e^{-p_f(y'+2t)} + R_{+}^{(2)}\, e^{p_f(y'-2t)}\right) dy'$$

and

$$w_{xf}^{r-} = \int_{-\infty}^{+\infty} \frac{j_x(y',\zeta)}{2j\omega\varepsilon_f p_f} \left(R_{-}^{(1)} e^{-p_f(y'+2t)} + R_{-}^{(2)}\, e^{p_f y'}\right) dy'$$

APPENDIX D

APPENDIX D

We would like to evaluate $\int_{C_p^+} \frac{d\zeta}{\zeta+\zeta_p}$. That is, we want to perform integration around the upper half plane surface wave pole. We make a change of variables such that

$$\zeta+\zeta_p = \varepsilon\ e^{j\varphi}$$

hence

$$d\zeta = j\varepsilon\ e^{j\varphi} d\varphi$$

where the contour around $\zeta = -\zeta_p$, ε and φ are shown in Figure 23. Therefore we have

$$\int_{C_p^+} \frac{d\zeta}{\zeta+\zeta_p} = - \int_{\pi}^{\pi} \frac{j\varepsilon\ e^{j\varphi}}{\varepsilon\ e^{j\varphi}}\, d\varphi$$

$$= -2\pi j$$

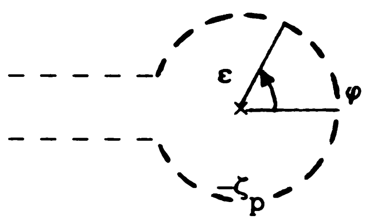

Figure 23: Evaluation of integration around the pole.

APPENDIX E

APPENDIX E

Symmetric Slab Specialization

In order to recover Rozzi's result, we must shift the y-axis as shown in Figure 24. It will be shown that both the discrete and the continuous part of the Green's function specialize to Rozzi's for the symmetric slab waveguide. For this case $p_s = p_c$, hence the coefficients $B_1(\zeta_p)$, $B_2(\zeta_p)$ and $B_3(\zeta)$ in the expression of the discrete Green's function in Chapter Three become

$$B_1(\zeta_p) = \frac{-j\gamma}{4\zeta_p(2+\gamma t)}$$

$$= B_3(\zeta_p)$$

$$B_2(\zeta_p) = \frac{j(jK-\gamma)^2\gamma}{4\zeta_p(2+\gamma t)}$$

From Figure 24, we define $\tilde{y}$ such that $y = \tilde{y} - t/2$. We also let $t/2 = d$. By doing so, the discrete Green's function becomes

$$\begin{aligned} G_{pole} = -2jk_0Z_0 \Bigg\{ & \Big[B_1(\zeta_p) + B_2(\zeta_p)(\cos 2Kd - j\sin 2Kd)\Big] \Big[\cos K\tilde{y}\ \cos Ky'\ \cos Kd \\ & - \cos K\tilde{y}\ \sin Ky'\ \sin Kd\Big] \\ & + \Big[B_2(\cos 2Kd - j\sin 2Kd) - B_1\Big]\Big[\sin K\tilde{y}\ \sin Ky'\ \cos Kd \\ & + \sin K\tilde{y}\ \cos Ky'\ \sin Kd\Big]\Bigg\} e^{-j\zeta_p|z-z'|} \end{aligned}$$

We use the eigenvalue equation as in Chapter Three specialized for the symmetric slab

$$\tan(2Kd) = \frac{-2\gamma K}{\gamma^2 - K^2} \tag{1}$$

to evaluate cos(2Kd) and sin(2Kd). We found

$$\cos(2Kd) = \frac{K^2-\gamma^2}{k_f^2-k_c^2} \tag{2}$$

and

$$\sin(2Kd) = \frac{2\gamma K}{k_f^2-k_c^2} \tag{3}$$

Using (1) and (2) in the expression of G_{pole} and the fact that $\tilde{y}' = y' + t/2$, we have

$$G_{pole} = \frac{k_0 Z_0 \gamma}{2\zeta_p(1+\gamma d)} \cos(K\tilde{y}) \cos(K\tilde{y}') \, e^{-j\zeta_p|z-z'|} \tag{4}$$

In Rozzi's result, the discrete Green's function is expressed as

$$G_{pole}(\tilde{y}|\tilde{y}';z-z') = -A^2 e_{xo}(\tilde{y}) \, e_{xo}(\tilde{y}') \, e^{-j\zeta_p|z-z'|} \tag{5}$$

where

$$e_{xo}(\tilde{y}) = A \cos(K\tilde{y})$$

and

$$A^2 = \frac{k_0 Z_0}{2\zeta_p \left[\dfrac{\cos^2(Kd)}{\gamma} + d + \dfrac{\sin(2Kd)}{2} \right]}$$

Using (1} and (3), $\cos^2(Kd)$ is found to be

$$\cos^2(Kd) = \frac{K^2}{\gamma^2+K^2} \tag{6}$$

By substituting (3) and (6) in the expression for A, we have

$$A^2 = \frac{k_0 Z_0 \gamma}{2\zeta_p (1+\gamma d)}$$

With the above expression for A^2, G_{pole} in (4) will be the exact replica of (5).

Similarly, the radiation Green's function of Rozzi's is the exact replica of our specialized continuous Green function. In fact, Rozzi's results are

$$G_R(\tilde{y}|\tilde{y}';z-z') = -\int_0^\infty \frac{Z_{TE}(\rho)}{4} e_{xo}(\tilde{y},\rho)\, e_{xo}(\tilde{y}',\rho)\, e^{j\zeta(\rho)|z-z'|}\, d\rho$$

$$-\int_0^\infty \frac{Z_{TE}(\rho)}{4} e_{XE}(\tilde{y},\rho)\, e_{XE}(\tilde{y}',\rho)\, e^{j\zeta(\rho)|z-z'|}\, d\rho$$

where

$$e_{XE}(\tilde{y},\rho) = \frac{A}{C}\cos(\sigma\tilde{y})$$
$$e_{xo}(\tilde{y},\rho) = \frac{A}{\tilde{C}}\sin(\sigma\tilde{y})$$

and

$$A = \sqrt{2/\pi}$$
$$\sigma(\rho) = \sqrt{v^2+\rho^2}$$
$$v = \sqrt{n_f^2-n_c^2}\; k_0$$
$$C(\rho) = \sqrt{1+(v/\rho)^2\sin^2\sigma d}$$
$$\tilde{C}(\rho) = \sqrt{1+(v/\rho)^2\cos^2\sigma d}$$

$$Z_{TE} = \frac{-k_0 Z_0}{\zeta(\rho)}$$

$\zeta(\rho)$ is defined as in chapter three for the second integral term.

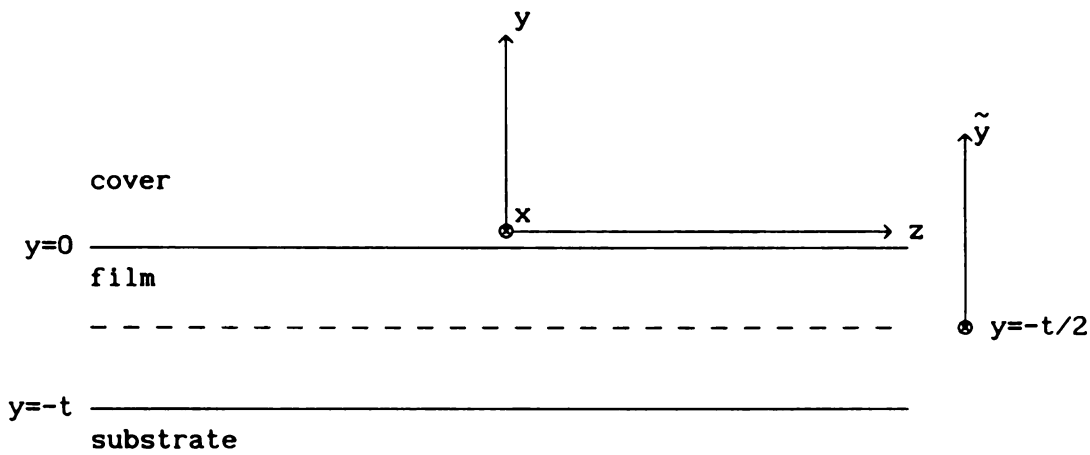

Figure 24: Symmetric slab specialization leading to $\tilde{y} = y + t/2$.

LIST OF REFERENCES

LIST OF REFERENCES

[1] T.E. Rozzi,"Rigorous analysis of the step discontinuity in a planar dielectric waveguides,"IEEE MTT Trans.,vol.26,pp.738-746 oct.1978.

[2] S.V. Hsu and D.P. Nyquist,"Integral-operator formulation for scattering from obstacles in dielectric optical waveguides," in Digest of the U.S National Committee/International Union of Radio Science Meeting (National Academy of Sciences, Washington, D.C.,1979),p.90.

[3] S.V. Hsu and D.P. Nyquist,"Integral-equation formulation for mode conversion and radiation from discontinuity in open boundary waveguide,"in Digest of the U.S National Committee/International union of Radio Science Meeting (National Academy of Sciences, Washington, D.C,1980),p.62.

[4] N.K. Uzunoglu,"Scattering from inhomogeneities inside a fiber waveguide,"Opt.Soc.Am.,vol.71,No.3,March 1981.

[5] P.G. Cottis and N.K. Uzunoglu,"Analysis of longitudinal discontinuities in dielectric slab waveguides,"Opt.Soc.Am.,vol.1, No.2,Feb.1984.

[6] T.G. Livernois and D.P. Nyquist,"Integral-equation formulation for scattering by dielectric discontinuities along open boundary dielectric waveguides,"Opt.Soc.Am,vol.4,pp.1289,July 1987.

[7] A. Sommerfeld,"Ueber die Ausbreitung der Wellen in der drahtlosen Telegraphie,"Ann.Physik,vol.28,pp.665,1909.

[8] J.S. Bagby and D.P. Nyquist,"Dyadic Green's function for integrated electronic and optical circuits,"IEEE MTT-S Tran.,vol.MTT-35, pp.206-210,Feb 1987.

[9] A. Sommerfeld, Partial differential Equations in Physics,New york: Academic Press,pp.236-265,1965.

[10] H.F. Weinberger, A First Course in Partial Differential Equations, New york: John Wiley and Son,Inc.,1965.

[11] R.E. Collin, Field Theory of Guided Waves, New york: Mc Graw Hill, pp.485-488,1960.

[12] D. Marcuse, Light transmission Optics, Princeton, N.J: Van

Nostrand Reinhold, chap. 9.

[13] D. Marcuse, Theory of Dielectric Optical Waveguides, New York: Academic, chap. 3, 1974.

[14] T.E. Rozzi and G.H. In't Veld, "Field and network analysis of interacting step discontinuities in planar dielectric waveguides," IEEE MTT Tans., vol. MTT-27, pp. 303-309, 1979.

[15] R.F. Harrington, Time Harmonic Electromagnetic fields, New York: Mc Graw Hill, pp. 125-128, 1961.